

DRAFT FINAL REPORT

**Structural Stability Assessment and Development of Design
Guidelines for Expanded Polystyrene Core Panel System
towards Safe and Affordable Housing**

Submitted to

Building Materials and Technology Promotion Council (BMTPC)

MoHUPA, Govt. of India, New Delhi



**Department of Earthquake Engineering
Indian Institute of Technology Roorkee
Roorkee, Uttarakhand – 247 667**

December - 2016

Contents

	Title	Page No.
	Contents	i
	List of Figures	iii
	List of Tables	vii
	Executive Summary	1
Chapter 1	Introduction	5
	1.1 General	5
	1.2 Sandwich composite panels	6
Chapter 2	Current Status: Literature Review	11
	2.1 Introduction	11
	2.2 Behaviour of sandwich panels	11
	2.3 Studies on compression behavior	12
	2.4 Studies on shear behavior	14
	2.5 Studies on flexural behaviour	15
	2.6 Studies on behaviour under lateral dynamic/seismic loading	17
Chapter 3	Study on Small Specimens: Experimental and Analytical Investigations	21
	3.1 Introduction	21
	3.2 Experimental programme	21
	3.2.1 Diagonal compression test	21
	3.2.2 Flexure test	42
Chapter 4	Seismic Analysis of A Sandwich Wall Panel Building	55

4.1 Introduction	55
4.2 Building specifications	55
4.3 Material specification	56
4.4 Finite element modelling	57
4.5 Pier analysis	59
4.6 Finite Element Analysis	62
4.7 Stresses in walls	63
4.8 Comparison of FEA results with pier analysis	65
4.9 Capacity and demand at the critical sections	66
4.10 Non-linear static pushover analysis	69
Chapter 5 Design Guidelines	73
5.1 Introduction	73
5.2 Design of wall panels for Compression	73
5.2.1 Pure axial compression in solid panels	73
5.2.2 Axial compression in panels with opening	74
5.3 Axial force-moment interaction	75
5.4 Shear capacity	80
5.5 Seismic design parameters	83
5.6 Fire and Durability	83
Chapter 6 Conclusions and Future scope of work	85
6.1 Conclusions	85
6.2 Future scope of work	86
References	87

List of Figures

Figure No.	Title	Page No.
Figure-1.1	Typical cross-section of RCSP sandwich panel	7
Figure-1.2	Isometric view of typical cross-section of RCSP sandwich panel	7
Figure-1.3	Schematic sketches of the components of wall and floor sandwich panels	7
Figure-1.4	Wall panel	7
Figure-1.5	Slab panel	7
Figure-1.6	EPS core with steel wire mesh and truss web connectors	8
Figure-1.7	Staircase panel	8
Figure-2.1	Stress distribution in sandwich panel systems due to pure bending	12
Figure-3.1	Schematic diagram of diagonal compression test: (a) Test setup; (b) Cross section of specimen; and (c) Details of specimen	22-23
Figure-3.2	Grain size distribution for mortar mix: (a) Range; and (b) As obtained	23-24
Figure-3.3	EPS panel	24
Figure-3.4	Seiving of Material	24
Figure-3.5	Sieved Aggregate, course sand, stone dust ,cement and reinforcement	25
Figure-3.6	Concrete Mixer	25
Figure-3.7	Air Compressor	25
Figure-3.8	Spray gun with hopper	25
Figure-3.9	Measurment for cutting EPS panel to the required size and shape	26
Figure-3.10	Prepared EPS panel for specimen	26
Figure-3.11	Palcement of U-bars at corners	26
Figure-3.12	EPS panel with U-bars reinforcement in corners	26
Figure-3.13	Assembling of casting frame	26
Figure-3.14	Checking of EPS specimen	27

Figure-3.15	Specimens ready for shotcreating	27
Figure-3.16	Preparation and application of cement slurry on specimen	27
Figure-3.17	Application of concrete on face of specimen through spray	27
Figure-3.18	Cleaning of corners using air-blast before filling	28
Figure-3.19	Filling of corners	28
Figure-3.20	Prepared specimen for diagonal compression test	29
Figure-3.21	Test setup for diagonal compression test	30
Figure-3.22	Date of casting and date of test	30
Figure-3.23	Loading Shoes for diagonal compression test	30
Figure-3.24	Cracking of specimen during diagonal compression test	30
Figure-3.25	Load-displacement curve obtained from diagonal compression test for specimens DC-1 to DC-3	31
Figure-3.26	Stress-strain curve of concrete used for analysis in SAP 2000	32
Figure-3.27	Stress-strain curve of steel wire mesh used for analysis in SAP 2000	33
Figure-3.28 (a)	Details of mesh, loading and boundary conditions in FE model in SAP 2000	33
Figure-3.28 (b)	Crack pattern observed in FEM analysis in SAP 2000	33
Figure-3.29	Load-displacement curve from simulation of diagonal compression test obtained from SAP 2000	34
Figure-3.30	Stress-strain curve of concrete in compression	35
Figure-3.31	Stress-strain curve of concrete in tension	36
Figure-3.32	Inelastic stress-strain curve of concrete in compression	37
Figure-3.33	Inelastic stress-strain curve of concrete in tension	37
Figure-3.34	Compression damage of concrete	38
Figure-3.35	Tension damage of concrete	38
Figure-3.36	Stress-strain curve of welded wire mesh	39
Figure-3.37	Model showing the three components of the EPS core panel	40
Figure-3.38	Details of loading applied and boundary conditions	40
Figure-3.39	Details of finite element mesh	40
Figure-3.40	Crack pattern obtained from analysis	40

Figure-3.41	Load-displacement curve obtained from nonlinear FE analysis in ABAQUS	41
Figure-3.42	Comparative study of numerical analysis and experimental results	41
Figure-3.43	Schematic diagraph of flexural test: (a) Test setup; (b) Reinforcement details of specimen; and (c) Cross section of specimen	43
Figure-3.44	Fabrication of form for casting of flexural test specimen	44
Figure-3.45	Finished form for casting	44
Figure-3.46	EPS panel for flexural test	44
Figure-3.47	Edge beam reinforcement and beam cage	45
Figure-3.48	Prepared EPS panel before casting specimen	45
Figure-3.49	Construction of EPS panel for flexural test	45-46
Figure-3.50	Casting of edge beam	46
Figure-3.51	Prepared specimen for flexural test	47
Figure-3.52	Test setup and loading arrangement for flexural strength test	48
Figure-3.53	Load-displacement curves of flexural test for specimens FL-1 to FL-3	48
Figure-3.54	Cracks at the mid-span and along the line of application of load	48
Figure-3.55	Loading, boundary conditions for flexure test in SAP 2000	49
Figure-3.56	Deflected shape due to flexure loading in SAP 2000	49
Figure-3.57	Load-displacement curve obtained for simulation of flexure test in SAP 2000	50
Figure-3.58	Diagram showing components of the FE model developed in ABAQUS for simulation of flexure test	50
Figure-3.59	Finite element mesh for simulation of flexure test	51
Figure-3.60	Loading and boundary conditions applied for flexure test	51
Figure-3.61	Deflected shape of the panel showing tension damage	51
Figure-3.62	Deflected shape, upside down condition to show the tension damage at the bottom	52
Figure-3.63	Load-displacement curve of four-point loading test as developed in ABAQUS	52

Figure-3.64	Load versus displacement curves obtained from experiment and finite element analysis	53
Figure-4.1	Plan of the building	57
Figure-4.2	Isometric view of the model developed in SAP 2000	58
Figure-4.3	Schematic diagram showing different piers in a typical load bearing wall, for use in pier analysis method	60
Figure-4.4	Stresses in wall A-A due to the most critical load combination: a) Vertical b) Shear stress	63
Figure-4.5	Stresses in wall B-B due to the most critical load combination: a) Vertical b) Shear stress	64
Figure-4.6	Stresses in wall C-C due to the most critical load combination: a) Vertical b) Shear stress	64
Figure-4.7	Stresses in wall D-D due to the most critical load combination: a) Vertical b) Shear stress	65
Figure-4.8	Stress-strain curve of concrete used for estimating capacities of sections	67
Figure-4.9	Stress-strain curve of steel wire-mesh used for estimating capacities of sections	67
Figure-4.10	Schematic diagram showing the critical section cuts of wall C-C marked in the plan view of the building	68
Figure-4.11	P-M interaction curves of a few critical sections showing demand forces	68
Figure-4.12	Deflected shape of the building with: (a) beam-column foundation; and (b) raft foundation	70
Figure-4.13	Capacity (Pushover) curves of the building in X-direction	71
Figure-4.14	Capacity (Pushover) curves of the building in Y-direction	71
Figure-5.1	Variation of strain and stresses on a composite panel cross-section subjected to eccentric axial loading	77

List of Tables

Table No.	Title	Page No.
Table 3.1	Material properties used in SAP 2000 model for diagonal compression test	32
Table 3.2	Parameters used for concrete damage plasticity model	39
Table 4.1	Comparison of pier analysis and finite element analysis (FEA) results for shear force in X-direction walls due to earthquake forces in X-direction	66
Table 4.2	Roof drift (%) at performance points	72
Table -5.1	Shear capacity of section without shear reinforcement (c) N/mm ² (IS 456, 2000)	81
Table -5.2	Maximum shear stress at section (c_{max}) N/mm ²	81

EXECUTIVE SUMMARY

The Ministry of Housing & Urban Poverty Alleviation (MoHUPA), Govt. of India, has launched an ambitious mission of “Housing for All (HFA) by 2022”. It is estimated that 2 Crore houses are to be constructed under this mission by 2022. It is difficult to achieve the ambitious target of the mission using conventional building materials (e.g. burnt clay bricks, stones, concrete blocks, timber, reinforced concrete, steel, etc.). Conventional building materials have finite resources and severe environmental impact. To achieve the target of the mission, there is need to develop construction systems which are quick, cost effective, disaster resilient and durable.

Building Materials and Technology Promotion Council (BMTPC), under the aegis of the MoHUPA has identified some emerging technologies, which have potential for large scale application to achieve the target of HFA mission. A ‘Technology Sub-mission’ has been created to help the HFA mission and MoHUPA in further developing and implementing the identified technologies. One of the emerging technologies identified by the BMTPC is ‘Expanded Polystyrene (EPS) Core Panel System’. It is a promising technology with potential for large scale application and a few vendors have already started production and construction of these houses in the country. However, adoption of this technology at large scale is hindered due to lack of the knowledge and confidence about the mechanical behavior, disaster resistance, and durability of this material. Towards this objective, BMTPC entrusted the Department of Earthquake Engineering, Indian Institute of Technology Roorkee, with a preliminary study on ‘Structural Stability Assessment and Development of Design Guidelines for Expanded Polystyrene Core Panel System towards Safe and Affordable Housing.’

An experimental study on mechanical behavior of EPS core based RC sandwich panels is conducted. Small scale wall specimens are constructed using the EPS core, galvanized wire-mesh reinforcement, and micro-concrete (structural plaster), and tested for the in-plane shear capacity and out-of-plane flexural behavior. The EPS panels have been



provided by M/S Schnell Homes (India) and the thicknesses of core (80 mm) and outer concrete layers (35 mm each) recommended by them has been considered. The wire reinforcement size (3 mm) and arrangement has also been used as per their manufacturing standards. The outer concrete layers were sprayed using a pneumatic spray gun. The composition and water-cement ratio of the concrete mix has been adopted to get the desired workability for spray application and to achieve the targeted strength of M25. The diagonal compression tests are performed as per the ASTM E519/E519-15 specifications to evaluate the shear strength of the panels and out-of-plane bending tests have been performed using four-point loading arrangement. The strength estimated using these tests has been compared with that using the Indian and other codes for ordinary reinforced concrete panels. It is observed that in absence of more rigorous models for EPC-RC composite panels, the models available in codes can be used for estimating the strength with reasonable conservativeness.

The small scale shear and flexure tests have been simulated using Finite Element Analysis. Two models, first using layered shell elements in SAP 200 Nonlinear software and the other using solid (brick) elements for concrete and truss (bar) elements for the reinforcement in ABAQUS have been used. The properties of constituent materials have been specified as obtained by the tests or by earlier researchers. It is observed that the solid element model in ABAQUS yields reasonably accurate simulation of the experimentally obtained load-deflection curve in diagonal compression, but the layered shell element model over-estimates the capacity. In case of the out-of-plane flexure test, initial portion of the load-deflection curve obtained from finite element analysis in ABAQUS matches with the experimental curves, but the latter part of the curves does not match as de-bonding occurred in the tested specimen whereas de-bonding failure has not been considered in the finite element model. The load-displacement curve of the finite element model shows significant strain hardening after the tensile failure of concrete as the steel has not yielded yet and the panel still has the load-carrying capacity. The experimental curve becomes flat after the steel yields and continues till the ultimate strain is reached. The results of



modelling using layered shell element in SAP 2000 show higher stiffness and strength in comparison to the experimental results.

In addition to the simulation of tests on small scale specimens, detailed analysis of a proposed 4 storey (G+3) building has been performed to study its seismic capacity. The building is proposed to have walls consisting of 100 mm thick EPS core and 60 mm thick concrete overlays (total thickness of the walls equal to 220 mm) and slabs having 160 mm thick EPS core, sandwiched between two layers of concrete, upper concrete layer thickness being 50mm and bottom concrete layer thickness being 30mm. The building is founded on columns and beams up to the plinth level and the sandwich panels are anchored to the foundation beams using steel dowels. Two types of analysis have been performed. First a simple ‘pier analysis’ is performed considering idealized modelling of piers as fixed end vertical frame elements and assuming the spandrels to be rigid. In the second case, a finite element model using layered shell element has been developed in SAP2000 Nonlinear software. The pier analysis is used to estimate the equivalent axial force, bending moment, and shear force in the piers, whereas the finite element model is used estimate the stresses and stress resultants in different components and for performing a nonlinear static (pushover) analysis.

The axial force, bending moment and shear force acting on the critical sections under all the considered load combinations are compared with the capacity. It is observed that the load carrying capacity of the sections is greater than the demand on the sections. The results of analysis conclude that the design of the building is adequate to withstand the earthquake forces. Further, the nonlinear analysis shows that the drift demand, in case of the EPS-RC sandwich building is much smaller in comparison with the conventional building systems and is also much lower, even under MCE, than the capacity. This is mainly due to the much reduced seismic weight of the EPS core building, in comparison with the conventional building systems.

Thus, the tests and analysis performed in this study demonstrate that the EPS core based RC sandwich panel system is a viable construction system for seismically safe buildings.



This report also provides some modelling guidelines, based on the available literature, for design of such buildings.

The study presented in this report has been performed as part of the Ph.D. work by Mr. Adil Ahmad, and an M.Tech. Dissertation by Mr. Avirup Sarkar, under the supervision of Prof. Yogendra Singh at Department of Earthquake Engineering, IIT Roorkee. Valuable inputs have been received from Dr. Shailesh Agrawal, Executive Director and Mr. J.K. Prasad, Chief, Building Materials, BMTPC. The financial support received from BMTPC for conducting the study is gratefully acknowledged. The support received from M/S Schnell Homes in the form of EPS panels, free of cost, and valuable discussions with Mr. Rajiv Singal and Ms. Lucia Manna, especially in design and preparation of the test specimens, is also gratefully acknowledged.

CHAPTER 1

Introduction

1.1 General

Economic growth of any country is evaluated by many parameters. Housing is one of such parameters, indicating development of a country. Affordable housing represents the financial and social power of the citizens of that country. As per census 2011, the rate of urbanization growth in India is 31.2%, it will further increase to 40% by 2020 (Vision 2020, planning commission) and 50% by 2041 (draft urban Indian report). Total shortage of housing dwellings in urban and rural areas is 101.75 million units. Keeping in mind the acute shortage of affordable housing in India, the Ministry of Housing & Urban Poverty Alleviation, Govt. of India, has launched an ambitious mission of **“Housing for All by 2022”**. The Mission predicts construction of 2 Crore (20 million) houses by 2022. To achieve this target, there is demand of time to have a construction system which is quick, cost effective, disaster resilient and durable; so that safe and affordable housing can be provided to the citizens of India.

To achieve the mission **“Housing for All by 2022”** by using conventional building materials (burnt clay bricks, stone blocks, timber, cement, sand, reinforcement etc.) and construction systems (load bearing walls, framed structures etc.) is a difficult tasks. Conventional building materials have finite resources. As the demand increases, there is direct (cost escalation) and indirect (rapid and irrational utilization) consequences. Further, it will lead to reduction in top fertile soil surface, deforestation and environmental degradation.

Lee, et al. (2006) have identified the characteristics of the ideal technologies for future construction industry, as affordability, energy efficiency, durability and safety, economically viable and beneficial, cultural acceptability, rapid applicability, adaptability, environmental sustainability, non-proprietary, easy maintenance, and reproducibility in



other markets. In view of these characteristics, the construction using cast-in-situ/precast reinforced sandwich panels and composite panels is a promising technique for future building construction.

1.2 Sandwich composite panels

In sandwich composite panels, generally there is one inner layer or ‘core’ of low strength material, which is protected by two outer layers known as ‘wythes’ of high strength skin materials. Reinforcement or wire-mesh may or may not be provided in skin layers. The thickness and type of core depend on its thermal resistance and design temperatures. The function of wythes is to provide load resistance, cover to reinforcement, anchorage to connectors, protection against stripping, and finish. Usually thickness of the wythes is less than the core. Two wythes are interconnected by shear connectors, webs, or combination of both. The function of shear connectors and webs is to hold the wythes and core in place, as well as to transfer the longitudinal shear in between wythes (Einea et al., 1991).

Use of sandwich panels in building construction industry was started in North America more than 60 years from now (PCI, 1997). Earlier sandwich panels were used as non-load bearing walls for partition and façade cladding. Recently, some construction companies started using these as load bearing structural elements.

This study is focused on the behaviour of sandwich panels constituted with inner core of Expanded Polystyrene (EPS) with shotcrete concrete and galvanized steel wire mesh reinforcement in two outer wythes. This type of sandwich panels are known as Reinforced Concrete Sandwich Panels (RCSP). Figures 1.1-1.7 show the schematic sketches of different types of wall, slab and staircase panels developed by different companies.

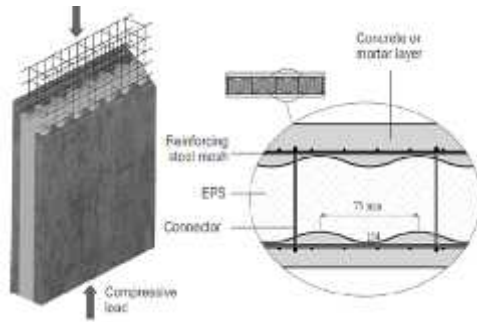


Figure-1.1 Typical cross-section of RCSP sandwich panel

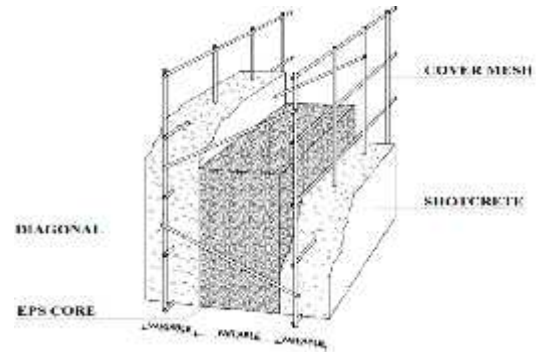


Figure-1.2 Isometric view of typical cross-section of RCSP sandwich panel

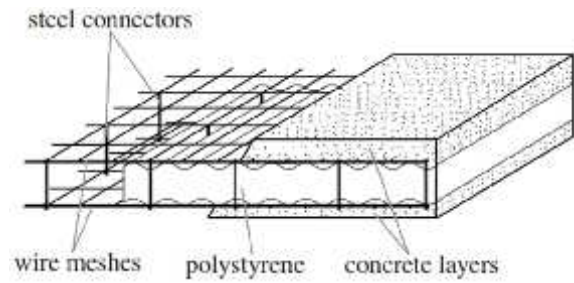
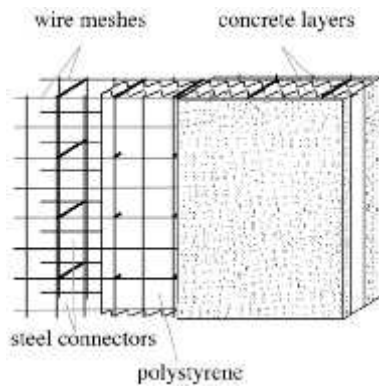


Figure-1.3 Schematic sketches of the components of wall and floor sandwich panels



Figure-1.4 Wall panel

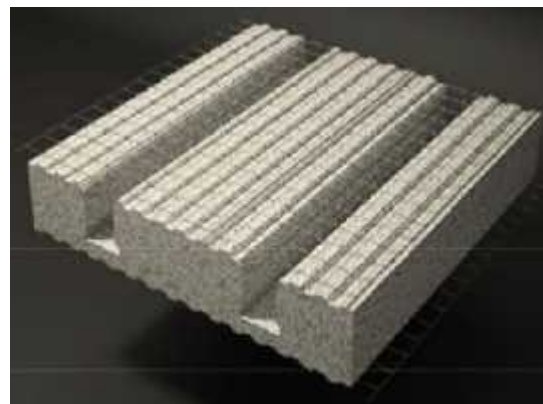


Figure-1.5 Slab panel



Figure-1.6 EPS core with steel wire mesh and truss web connectors



Figure-1.7 Staircase panel

Sandwich panels can be used to construct buildings with any geometry of walls, slabs and staircase. These provide quick, efficient and resilient building construction method. These have the following advantages over the conventional construction materials:

- Offers very high strength-to-weight ratio as well as stiffness-to-weight ratio, which enhances rigidity and strength without adding substantial weight.
- Offers high resistance against earthquake and wind forces.
- Light in weight and easy to handle and light foundation is required.
- Speedy in construction, as no shuttering is required.
- Flexibility in modifications and changes at later stage.
- Good heat, moisture and sound insulation properties, provided by the EPS core.
- Superior fatigue strength.
- Economical by avoiding formwork and skilled labour.
- Environment friendly, as it requires lesser material resulting in less severe impact on environment.
- Free from CFC and other toxic compounds.
- Offers improved blast resistance and safety against terror and sabotage activities.
- Reasonable fire rating (up to 60 minutes reported in the literature).

In view of the above properties, the RCSP is a very promising emerging construction technology to meet the ambitious tasks of the HFA mission. The main hurdle in large scale application of this technique, at the moment in India, is lack of design guidelines and



standardization for this system. This study reviews the available literature and test results from different parts of the world and explores the applicability of conventional design theories available for RC structures, to this type of constructions, which may be very useful in design of these buildings. In later part of this report, some experimental investigations to estimate the basic properties of RCSP elements and a feasibility study for a typical 4 storey building have been presented.



This page intentionally left blank

CHAPTER 2

Current Status: Literature Review

2.1 Introduction

The concept of sandwich panels was introduced in early 20th century in aviation, automobiles and ship industry. Applications of sandwich panels to construction and civil engineering purposes were very few. Only a few researches addressed to the structural use of sandwich panels (Fam and Sharaf, 2010). The behaviour of RCSP is complex due to material nonlinearity and the interaction between various components. To understand the behaviour of sandwich panels researchers are dependent on experimental investigation supported by simple analytical studies. Many sandwich panels used in North America and Europe are proprietary and publically available data is very limited (Benayoune et al., 2007). Some experimental, analytical, numerical and dynamic studies have been conducted globally to determine the mechanical properties of sandwich panels of different materials and configurations. However, there are not adequate guidelines for designing of sandwich panel buildings against gravity and seismic forces (Mousa, 2014). In this chapter, the main emphasis is on studies related to reinforced concrete sandwich panels (RCSP) to get the information about its behavior in compression, flexure, shear and dynamic loading, along with effects of earthquakes.

2.2 Behaviour of sandwich panels

Load carrying capacity of sandwich panels depends upon the composite action of wythes and longitudinal shear stress transfer mechanism by the connectors. If the applied flexural load is resisted by both wythes integrally, panel is **fully composite** and bending stress distribution will be continuous across the section, as shown in Figure 2.1(a). If the connectors are not capable of transferring full longitudinal shear stress, the panel will be **partial composite** panel and bending stress distribution will be as shown in Figure 2.1(b). A panel is said to be **non-composite** if the connectors have no capacity to transfer



longitudinal shear stress and bending stress distribution will be as shown in Figure 2.1(c) and 2.1(d) (Einea et al., 1991).

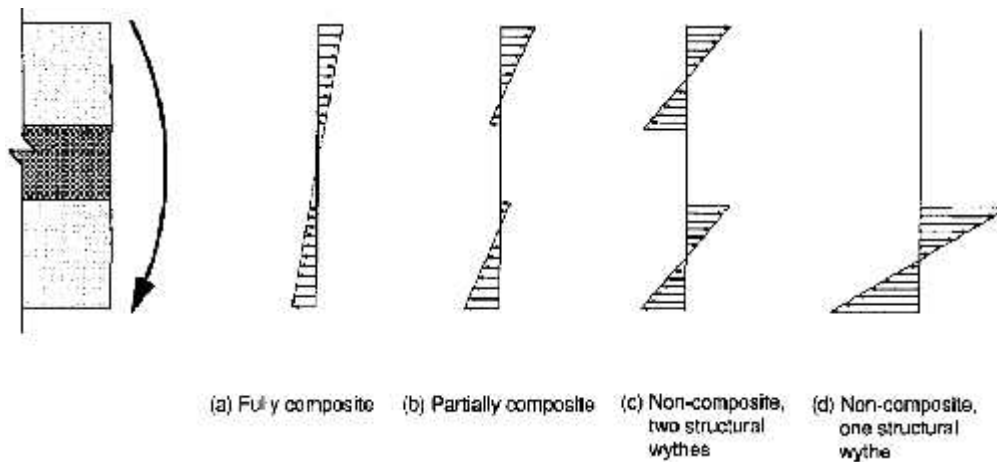


Figure 2.1 Stress distribution in sandwich panel systems due to pure bending

2.3 Studies on compression behavior

Benayoune et al. (2007) conducted full scale test under axial loading, on Precast Concrete Sandwich Panel (PCSP) of various slenderness ratios varying from 10 to 20. Violent failure occurred in all cases by crushing at either one or both ends of the panels. The first cracks were noticed to appear at loads of 44–79% of the ultimate loads. Strength reduction in axially loaded panels is less as compared to eccentrically loaded panels. The results obtained using ACI equation and expressions of other researchers for solid walls are conservative as compared to FEA and experimental results. They also proposed a semi-empirical formula for calculation of load carrying capacity. Gara et al. (2012b) tested sandwich panels, under vertical in-plane load. Numerical simulations were also performed with non-linear finite element models. Numerical simulations indicated that the ultimate loads of axially loaded panels are close to the buckling load whereas ultimate loads of eccentrically loaded panels are significantly lower than the buckling loads. The results of the experiments and numerical simulations indicated that a partial degree of composite behaviour was attained by the tested panels even if non-shear connectors are used in the interior layer.



Carbonari et al. (2013) presented a characterization of behaviour of Expanded Polystyrene (EPS) sandwich panels, with the variations in EPS thickness, mortar layer thickness and mixes, and panel height, through experimental results and proposed analytical formulation. Influence of length of connector provided through EPS thickness was observed and found that as the thickness increases, the load carrying capacity decreases. Increase in compressive strength of mortar enhances the load capacity, whereas mortar thickness did not cause any considerable effect. Height of panel played considerable role in load capacity of panel. The increase in length dimension produces considerable reduction in load capacity of panels. Maximum load is also affected by position of reinforcing mesh. The load resistance is maximum when the mesh is placed at center line of mortar.

Benayoune et al. (2006) tested full scale Precast Concrete Sandwich Panels (PCSP) of various slenderness ratios from 10 to 20 under eccentric load. It was observed that panels failed in crushing. The first crack occurred at 38-55% of failure load. As the slenderness ratio increases, the load carrying capacity decreases nonlinearly. FE analysis was also performed using commercial software LUSAS. FEM results and experimental results were in good agreement, while classical expression based on reinforced concrete principle underestimates the strength of the PCSPs.

Aziz et al. (2004) performed experiments on sandwich panels with openings and verified the theoretical ultimate load calculated using Saheb and Desayi (1990) equation for ordinary wall with opening. The average ratios of experimental to theoretical ultimate loads for sandwich panels were found to vary from 0.99 to 1.01.

Mohamad et al. (2011) tested sandwich panels of 40mm thick lightweight foamed concrete as wythes and polystyrene insulation of 20mm to 45mm thickness as core. Wythes were reinforced with 9mm diameter high tensile strength layer and 6mm dia. mild steel bars at 45° as shear connectors. The crack pattern has shown the failure due to local buckling in all the panels. Crushing occurred in all the cases at either one or both ends of the panel. The first crack was noticed to appear at loads of 51% to 72% of ultimate loads. Mousa and Nasimuddin (2011) presented study on a new type of composite structural insulated panels (CSIPs), made of low-cost thermoplastic orthotropic glass/poly-propylene (glass-PP)



laminated as a face sheet and expanded polystyrene foam (EPS) as a core with very high facesheet/core moduli ratio, under concentric and eccentric loading. CSIPs specimens failed by global buckling mode in which no de-bonding was observed. The eccentric specimens failed at load 35% lower than that of the concentric ones. Global buckling formulas for concentric and eccentric loading were presented and validated using the experimental results and were in a good agreement. An equivalent stiffness formula was also developed for sandwich wall under in-plane loading. Design graphs for global buckling were developed to be used as a preliminary design for CSIPs wall under concentric and eccentric loading.

2.4 Studies on shear behavior

Very few studies have been performed for determination of shear strength of sandwich panels. Shear strength of sandwich panels can be determined by either direct shear test or diagonal compression test. Kabir (2005) performed direct shear test on 550 mm height and 1000 mm long panel. FEM analysis with incremental loading, was also performed using ANSYS. For FE modeling of panel two types of elements were used. Non-linear 8-noded solid elements for concrete and beam elements for wythe steel and shear connectors were used. The load deflection curve is linear upto 6000kg and first crack occurs at 7000kg. The sample failed at ultimate load 12000kg and crack pattern is perpendicular to the normal principal stresses. Cracks occurred over the full length of sample and shear sliding was the failure mechanism. The panel's behaviour was same as a deep beam. Load deflection curve and ultimate load obtained from experiment and FEM analysis are matching.

Gara, et al., (2012b), performed diagonal compression tests to assess in-plane shear strength of EPS core wall panels. Three types of specimens were tested: simple wall panels, prestressed wall panels and panels with transversal stiffening walls. Diagonal compression tests were carried by means of a slide push by six hydraulic jacks. Panels with transversal walls show more deformation capacity than plane wall. Cracking load of prestressed panel is more as compared with other wall panels. In all tests, there was no sudden failure. The



numerical simulation was done with an elastic FEM model using SAP2000. Concrete was modelled with shell elements of thickness equal to total thickness of concrete. Experimental load deformation curve was compared with numerical model considering elastic modulus E_c and $0.4E_c$ to take into account cracking of concrete. Up to the first crack load of 100 kN, the experimental load-deformation curve matches with the numerically obtained curve for full value of E_c , and after cracking, the numerical curve with $0.4E_c$ simulates the experimental behavior well. Maximum value of horizontal tensile stress in central node reaches 2.3 N/mm^2 , nearly equal to ultimate tensile strength of concrete.

2.5 Studies on flexural behaviour

Experimental and analytical (FEM) studies were performed by Benayoune, et al. (2008) to understand flexural behaviour of precast concrete sandwich panels (PCSP). The observed crack pattern was similar to the conventional solid slab. First crack appeared at approximately 55%-60% of the ultimate load. Truss shaped shear connectors give substantial degree of composite action, and the diameter of shear connectors influences the ultimate strength and composite action. In FEM analysis, 2D and 3D models were proposed for one-way and two way slabs. In two way slabs, shear connectors were placed in both longitudinal and transverse directions, whereas in one way slabs, shear connectors were placed only in longitudinal direction. FEM analysis was done in software LUSAS using four types of elements: 3D thin shell element, 2D isoparametric plane stress element, 2D bar element and 3D bar element. In one way slab, concrete wythes were modelled using 2D isoparametric plane stress element and 2D bar elements were used to model shear connectors and reinforcement. Two way slabs were modelled using 3D thin shell element and 3D bar element. Experimental results are in good correlation with analytical study. Results obtained from 2D model are very close to experimental results. The difference is less than 4% in ultimate load and 1.5% in deflection in elastic range. In 3D modelling, the difference in ultimate load is 16% on higher side and 1.2% in deflection in elastic range. 2D model predicts reasonable value of strain in shear connectors. Accordingly, 2D model was recommended to evaluate the composite behaviour at elastic and ultimate states.



Bajracharya et al. (2012) have done structural evaluation of Concrete Expanded Polystyrene (CEPS) sandwich panels, as slabs, using FEM with 8-noded brick elements in software Strand7. 8-noded brick finite element model accurately predicted the load deformation behaviour. Carbonari et al. (2012) performed experiments to study the flexural behaviour of sandwich panel having 90° shear connectors. Three experiments were performed, one with simply supported and two with monolithic connections between walls and slab to simulate actual conditions. It was observed that connectors' contribution to stiffness of slab is small. The slab has high deformation and cracking under normal service load. Maximum load resisted by slab may be increased by changing shear connectors from 90° to incline. High deformation and cracking is related to failure of welding between steel mesh and connectors. Special attention must be paid to the welding between the connectors and the steel mesh embedded in the concrete layers.

Gara et al. (2012a) carried out test on simply supported floor panels and on wall-floor junctions. Numerical simulations with linear and non-linear FEM were also performed. A full scale 3D single story building was also tested to assess the ultimate capacity of real floor taking into account the wall-floor connections and bi-directional behaviour. Semi-composite behaviour was observed in flexural test panel due to low slip between concrete wythes and EPS core. A tri-linear behaviour with a very small uncracked phase was identified. Formulas for estimation of cracking and failure moment have also been proposed. Wall-floor junctions showed significant restraint against rotation and it depends on arrangement of wall and floor panels at junctions. Wall-floor junctions can be constructed in two different types, in the first type, floor panels cross the wall panels, and the wall panels were interrupted at the floor level. Whereas in the second type, floor panels are interrupted and wall panels are continuous. The first system has larger stiffness and strength as compared to the second system. The bending moment resisted by first system on a 1.12m wide panel is 7.73 kNm and second system resists only 4.63kNm. Waryosh et al., (2013) conducted test on sandwich panels made of light weight concrete as core and reinforced concrete as wythes, connected by truss type shear connectors. Experiments were conducted with three variables (thickness of core, strength of wythes and type of light weight concrete in core), keeping two variables as fixed and varying one at a time. Flexural strength increases with increase in thickness of panels. Flexural strength of panel with



sawdust as light weight aggregate in core is more than polystyrene and porcelenite. Central deflection decreases with increase in strength of the concrete used in wythes.

2.6 Studies on behaviour under lateral dynamic/seismic loading

Cantilever and fixed end reinforced concrete sandwich wall panels (RCSPs) with and without openings along with 2-storey full scale H-shaped walls were tested under simulated seismic loading by Pavese and Bournas (2011). All panels exhibited only a relatively gradual strength and stiffness degradation and in no case did any panel suffer from sudden shear failure. The study concluded that RCSP is a good construction system in high seismicity regions. Bournas et al. (2012) proposed a 'column model' for nonlinear analysis of RCSPs walls under cyclic loading. The model consists of an elastic column element with nonlinear flexural and shear springs concentrated at the column ends. It yields satisfactory results of flexural and shear forces in the global response of the walls if constitutive law is used properly.

Pseudo-static cyclic tests were performed by Ricci et al. (2013) on cast-in-situ sandwich panels with and without opening for determination of stiffness, strength, ductility, and energy-dissipation under seismic loading. For a drift of 0.1-0.2% damping ratio is slightly more than 0.05 and for drifts of 0.4-1.0% damping ratio is 0.1, and the ductility is in the range 5 to 8.5. The drift at yielding is approximately equal to 0.1%. Panels can withstand horizontal load up to inter-storey drift equal to 1.3% without loss of the vertical load-carrying capacity. Tested panels are able to withstand high horizontal loads, approximately equal to 100 kN/m. Seismic performance of the tested sandwich panels is comparable with those of common RC panels. Trombetti et al. (2012a) developed analytical model to evaluate mechanical characteristics and seismic behaviour of lightly reinforced concrete panels. Comparison between experimental results and analytical models has been performed. Experimental results were in good agreement with analytical model. Panels do show large values of kinematic ductility. The analytical tools developed for the seismic design can be successfully used for the actual seismic design of building structures.



Trombetti et al. (2012b) reported assessment of the seismic performance (stiffness, strength, ductility) of cellular structures built with lightly reinforced concrete/polystyrene sandwich panels. Horizontal loading cycles were imposed to the structures, while the vertical load was kept constant. It was observed that there is no real collapse, but just a “virtual collapse”. A good degree of kinematic ductility was developed. Sliding shear with pinched mode of failure was observed.

Rezaifar et al. (2008) conducted full scale dynamic test on single storey building constructed with sandwich panel, on shake table under several ground motions. The results obtained from experiment were also compared numerically using ANSYS. 3D panel buildings have considerable resistance to high levels of earthquakes due to: (i) over strength, (ii) minor energy dissipation by inelastic deformations, and (iii) the small drift. The overall displacement ratio of 4.5 and the over strength coefficient of approximately 6.0 were found using pushover analysis.

Ricci, et al., (2012), Ricci, et al., (2013b), Palermo, et al. (2014) performed shake table test on full scale 3-story building. The plan dimensions of building was 4.10m x 5.50m, height of building 8.25m and inter-storey height 2.75m, Figure 4.66. Construction of building was done using the sandwich panel of same specifications as used by authors in earlier papers. First the theoretical seismic capacity and expected mechanisms of failure was calculated. Three-dimensional FEM model was developed using SAP2000 to get modes of vibration and natural frequency. Modeling was done with shell-layered elements for both uncracked and fully cracked conditions, these conditions were simulated by taking different value of modulus of elasticity of concrete. For uncracked condition $E_{c,UC} = 25000\text{MPa}$ and for cracked condition $E_{c,FC} = 2750\text{MPa}$. The fundamental frequency of uncracked building was 12.8Hz and for cracked building was 3.3Hz. The expected sequence of failure of mechanisms with peak shaking table acceleration were identified. The test was performed on shake table with traditional instrumentation along with an advance instrument optical monitoring system. Acceleration Time history of Montenegro -1979 earthquake was used for seismic tests. White noise tests were performed before and after each seismic test in order to estimate the variation in the dynamic properties of prototype system. Spectrograms from white noise test were obtained and natural frequencies were presented. Up to five



white noise test (i.e. till PGA of 0.5g) fundamental frequency was constant, decrease in frequency was observed after PGA of 1.0g. The record of acceleration time history is similar to the previous papers of the authors. There was dynamic amplification of acceleration between bottom of table to top storey of the order of 1.4 to 1.7. Time history was recorded and it was found that the amplitude of strain in concrete is less than 0.5×10^{-3} . Displacement was recorded during the test. Inter-storey drift of 0.26% for first storey and 0.3% for roof was recorded. The first visible crack was observed at 1.0g PGA and were mostly concentrated around the openings. The response of shake table test was better than as anticipated by analytical calculations. The natural frequency calculated from FEM model and experiment is almost matching. The modules of elasticity required to match initial and final frequency are equal to 15000MPa, and 10,200 MPa. This indicates that, even after some cracks due to earthquake the building will perform similar to uncracked building. It was observed that the building is having over strength. The underestimation of strength may be due to neglecting tensile strength of concrete. The over strength of building is also explained by “Modified Compression Field Theory”, the peak shear strength of panel is approximately two times the ultimate strength.



This page intentionally left blank

CHAPTER 3

Study on Small Specimens: Experimental and Analytical Investigations

3.1 Introduction

Experimental and analytical studies have been conducted on small scale specimens of expanded polystyrene core based concrete sandwich panels to assess the mechanical properties of sandwich panels. Diagonal compression and flexural tests were performed and simulation was done using nonlinear layered shell elements in SAP2000 and nonlinear solid elements in ABAQUS software. Diagonal compression test was used to estimate the in-plane shear strength whereas the flexure test was used to determine out-of-plane strength of the sandwich panels.

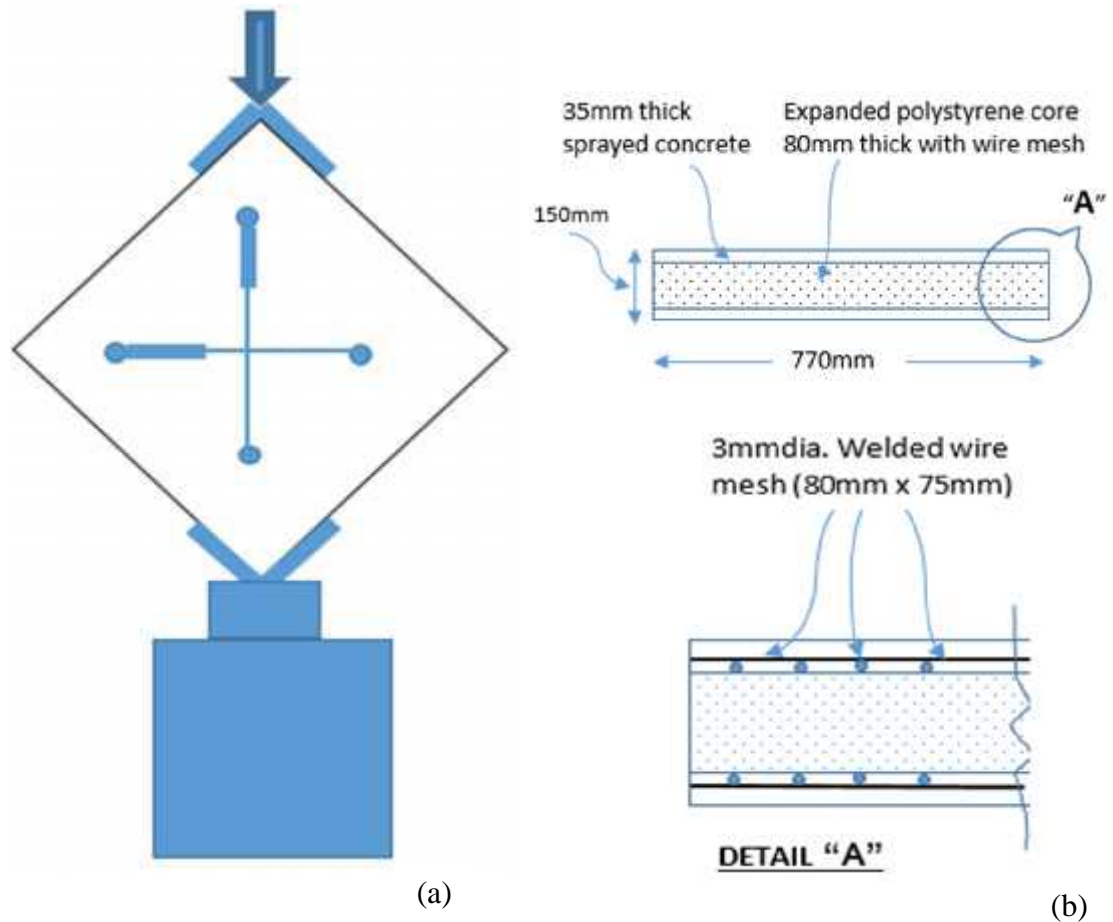
3.2 Experimental programme

3.2.1 Diagonal compression test

Diagonal compression test was performed on small scale specimens of sandwich wall panels of size 770mm x 770mm x 150mm. Specimens were prepared by using expanded polystyrene core of 770mm x 770mm x 80mm with welded wire mesh of 3mm dia. wire (80mm x 75mm mesh). The outer layers of concrete were 35mm thick. The grade of concrete was M25 and steel wire mesh has yield strength of 700 MPa. At the loading corners, the triangular portion of the EPS was removed and the corners were filled with concrete. In addition, 6 - #8mm, U- shape bars of 200mm length were provided to prevent the corner crushing under concentrated load. The U- shape bars were tied to the welded wire mesh to avoid displacement during concreting. Schematic diagram of sample and diagonal compression test is shown in Figure 3.1.



The concrete layers were applied by spraying the concrete (shotcrete) on the EPS core and wire mesh, on both the sides. The sprayed concrete was prepared by mixing coarse aggregate passing 4.75mm sieve, ordinary Portland cement, sand, stone dust, water and Gelenium plasticizer. Coarse aggregate, sand and stone dust were mixed in such a proportion that the grain size distribution curve lie in the range of curve as shown in Figure 3.2. The water-cement ratio was maintained 0.45-0.5.



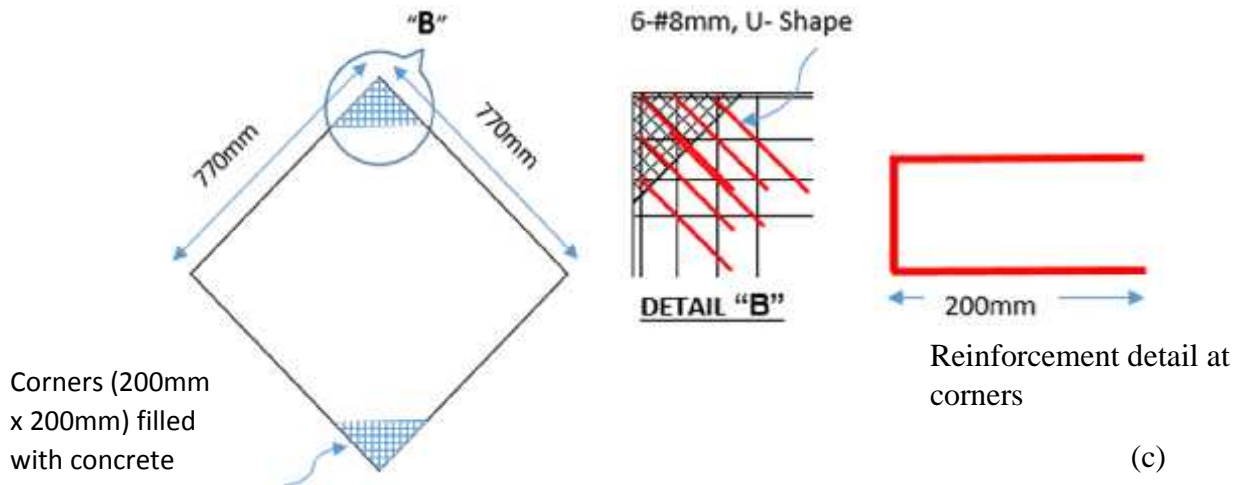
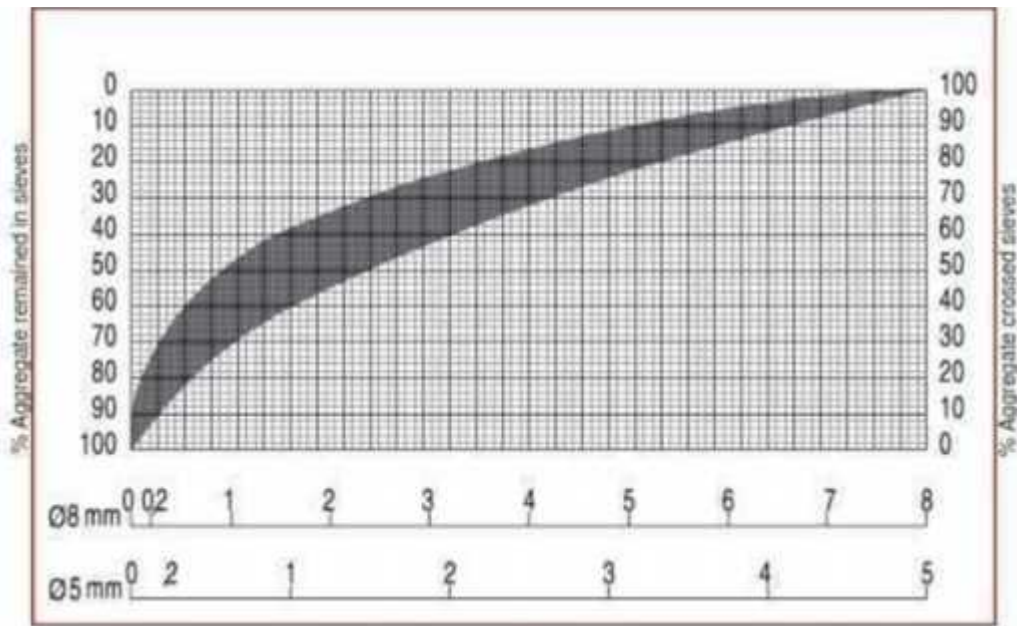


Figure 3.1 Schematic diagram of diagonal compression test: (a) Test setup; (b) Cross section of specimen; and (c) Details of specimen



(a)

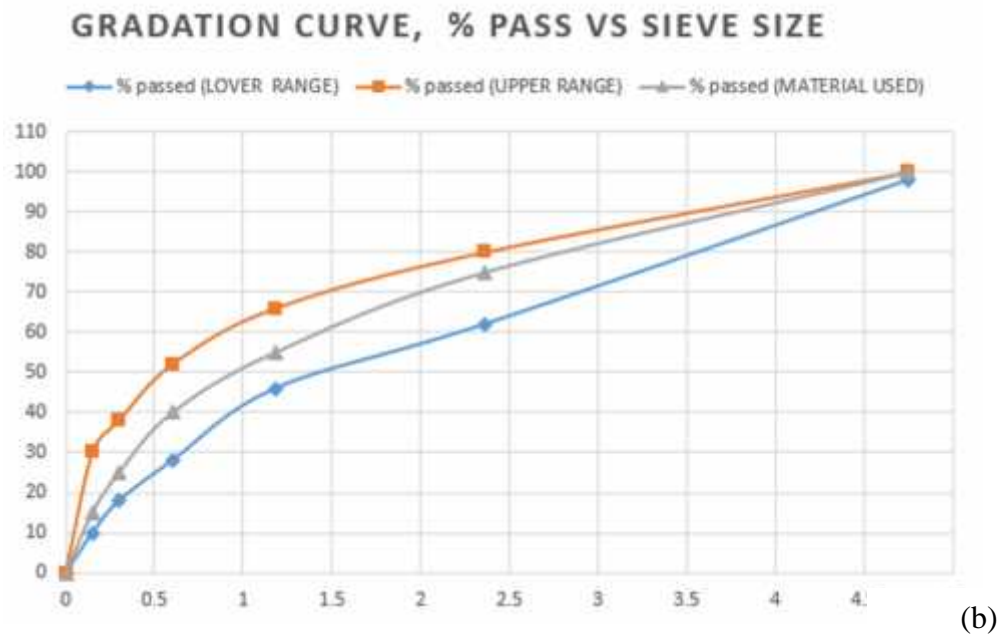


Figure 3.2 Grain size distribution for mortar mix: (a) Range; and (b) As obtained

Material used for construction of EPS sandwich wall panel specimens are shown in Figures 3.3 - 3.5. Preparation and spraying of concrete was done using the equipment like concrete mixer, spray gun and air compressor. Figures 3.6 - 3.8 show the equipment used for making of specimens. Figures 3.9 - 3.20 illustrate the preparation of specimens for diagonal compression test.



Figure 3.3 EPS panel



Figure 3.4 Sieving of Material



Figure 3.5 Sieved Aggregate, course sand, stone dust ,cement and reinforcement



Figure 3.6 Concrete Mixer



Figure 3.7 Air Compressor



Figure 3.8 Spray gun with hopper



Figure 3.9 Measurement for cutting EPS panel to the required size and shape

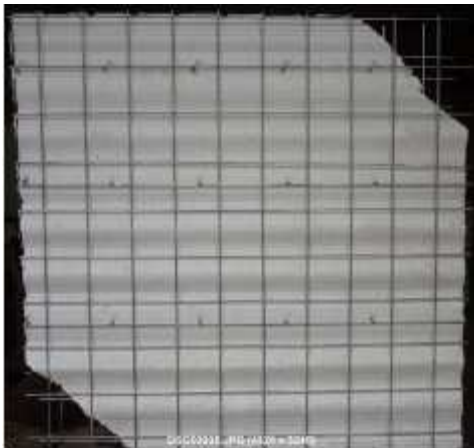


Figure 3.10 Prepared EPS panel for specimen



Figure 3.11 Placement of U-bars at corners



Figure 3.12 EPS panel with U-bars reinforcement in corners



Figure 3.13 Assembling of casting frame



Figure 3.14 Checking of EPS specimen



Figure 3.15 Specimens ready for shotcreting



Figure 3.16 Preparation and application of cement slurry on specimen



Figure 3.17 Application of concrete on face of specimen through spray



Figure 3.18 Cleaning of corners using air-blast before filling



Figure 3.19 Filling of corners



Figure 3.20 Prepared specimen for diagonal compression test

Total 03 specimens for diagonal compression test were casted at the Department of Earthquake Engineering IIT Roorkee. To investigate the in-plane shear behaviour of sandwich panels, diagonal compression tests were performed. ASTM E519/E519-15 standard procedure was followed to estimate in-plane shear strength of specimens. The diagonal compression load was applied on the opposite corners of the panels using the 250 T capacity INSTRON closed loop Universal Testing Machine (UTM), available at IIT Roorkee. The experimental setup for the diagonal compression test is illustrated in Figure 3.21 and 3.22. Displacement controlled diagonal loading was applied to the panel through a set of steel shoes (Figure 3.23) placed at top and bottom corners of the specimen. The rate of loading was kept 0.2 mm/min. The displacements of panel diagonals in compression and in tension were measured on a gauge length of 380 mm in the middle of specimen by two diagonally placed linear variable differential transducers (LVDTs) attached on opposite sides of the specimen. The LVDTs were directly attached to the specimen using a screw and clamp arrangement and connected to the same data acquisition system used for measurement of applied load, facilitating synchronized measurement of load and deformation. Cracks were developed along vertical direction i.e. parallel to loading direction Figure 3.24.



Figure 3.21 Test setup for diagonal compression test



Figure 3.22 Date of casting and date of test

Figure 3.23 Loading Shoes for diagonal compression test

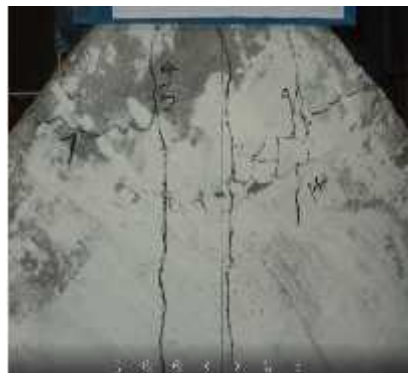


Figure 3.24 Cracking of specimen during diagonal compression test

Load deflection curves for three specimens are obtained from diagonal compression test as shown in Figure 3.25. The maximum diagonal force that is resisted by the three specimens are 246 kN, 257 kN and 269 kN respectively, after which softening behaviour is observed

in all the three cases and the ultimate displacement observed in the three specimens is in the range of 7mm to 10 mm.

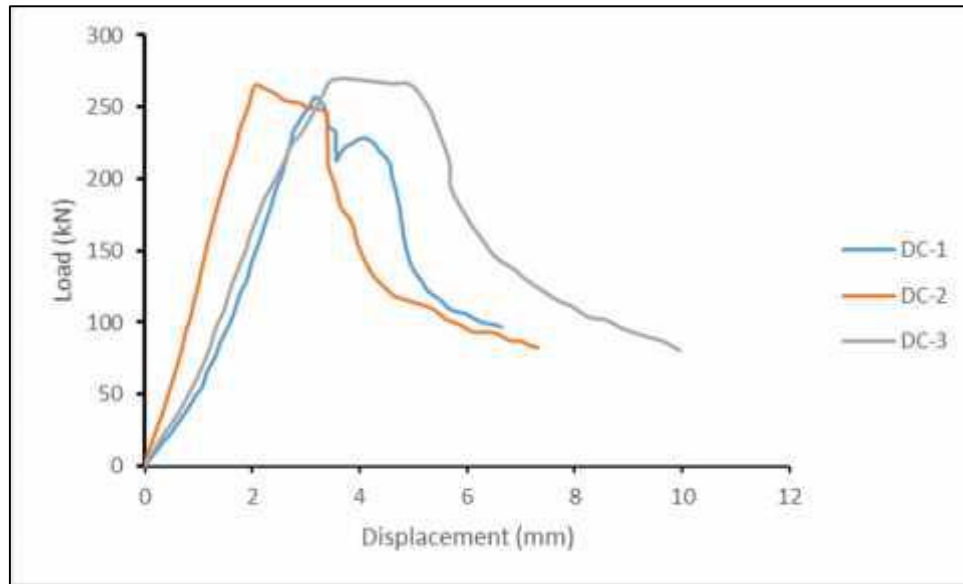


Figure 3.25 Load-displacement curve obtained from diagonal compression test for specimens DC-1 to DC-3

Numerical Simulation Diagonal compression test

Numerical Simulation diagonal compression test to obtain in-plane shear strength of the EPS core panels was done using SAP 2000 and ABAQUS. Sandwich panel of the same dimensions and configuration as tested, was modelled in SAP 2000 using layered shell elements. Steel wire mesh is embedded in each of the concrete layers. The basic properties of each of the component layers is provided in the Table 3.1. Stress-strain curve for concrete and steel used in modelling are shown in Figure 3.26 and 3.27, respectively. The layered shell element is a finite element formulation which behaves like a thick plate (Mindlin/Reissner) and takes into account transverse shear deformations. The schematic diagram of the model developed for the diagonal compression test in SAP 2000 is shown in the Figure 3.27.



Table 3.1 Material properties used in SAP 2000 model for diagonal compression test

Material	Density (kg/m ³)	Young's Modulus (MPa)	Poisson's Ratio
Concrete (M25 grade)	2400	25000	0.2
Expanded Polystyrene (EPS)	15	25	0.2
Welded Wire Mesh (f_y 700)	7850	200000	0.3

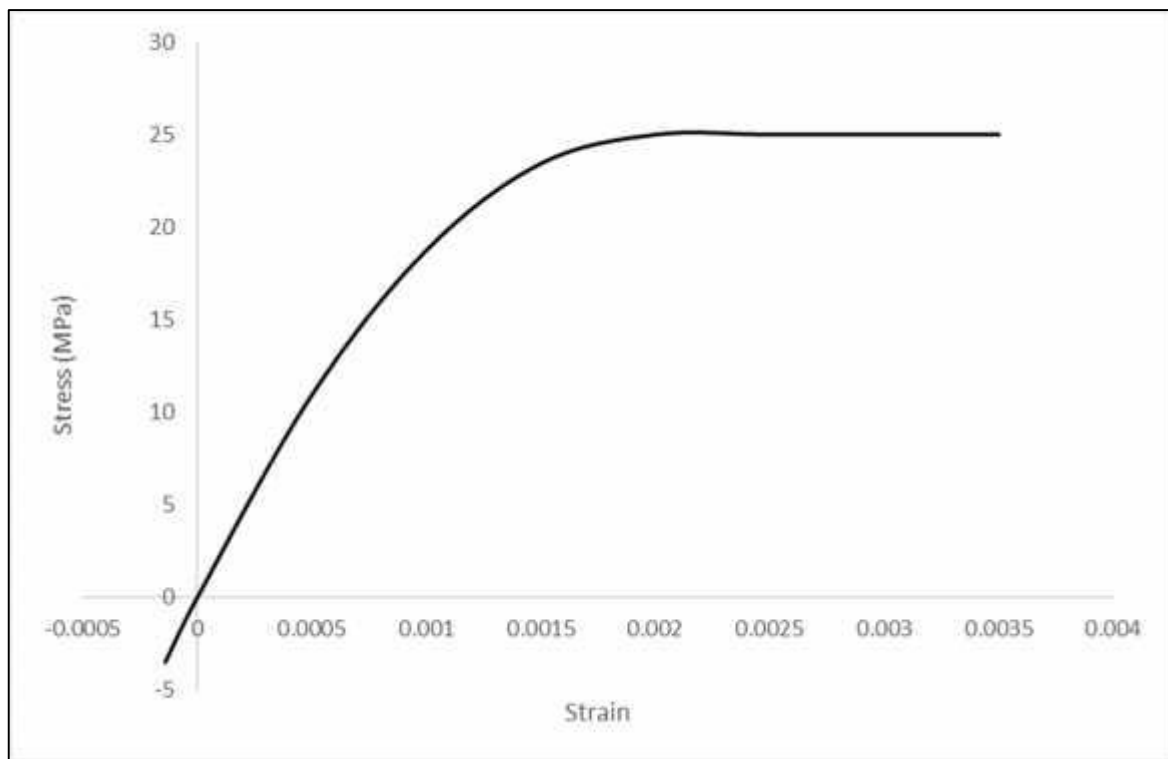


Figure 3.26 Stress-strain curve of concrete used for analysis in SAP 2000

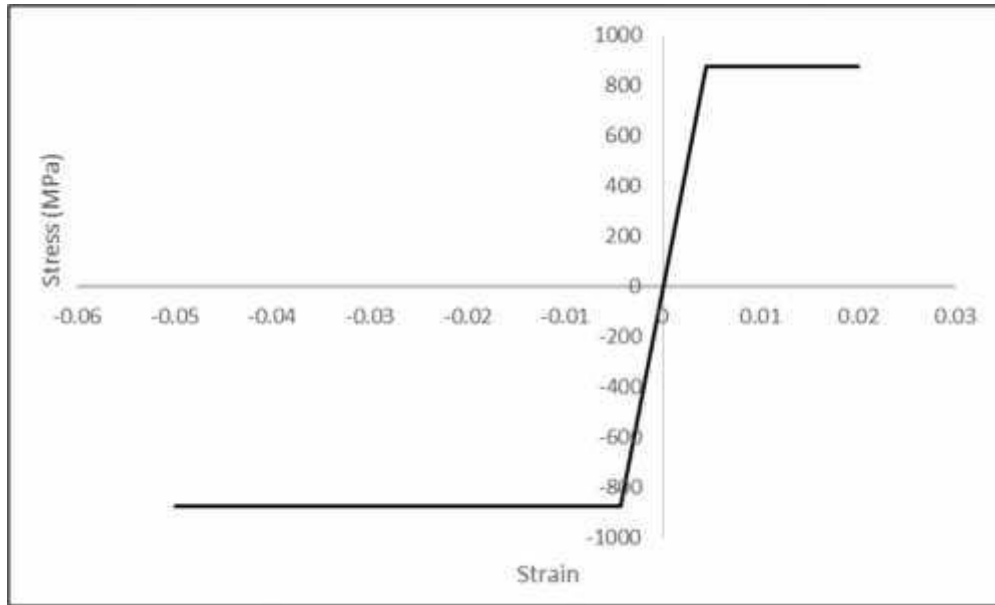


Figure 3.27 Stress-strain curve of steel wire mesh used for analysis in SAP 2000

Uniformly distributed load is applied at the top along the adjacent sides for a total length of 150 mm (the actual contact length in the experimental setup) and the same length is kept fixed at the bottom. Non-linear static analysis is performed by increasing the applied load (displacement) till failure occurs. Figure 3.28(b) shows crack pattern obtained from the nonlinear static analysis. The load-displacement curve obtained is shown in the Figure 3.29.

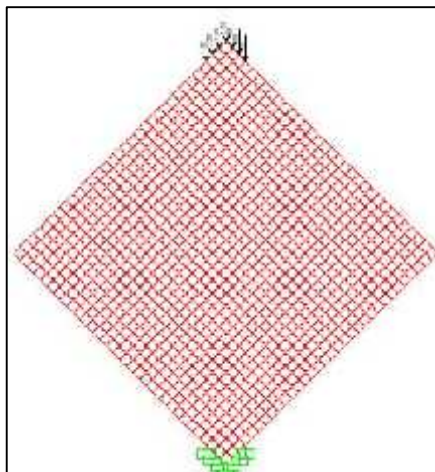


Figure 3.28 (a) Details of mesh, loading and boundary conditions in FE model in SAP 2000

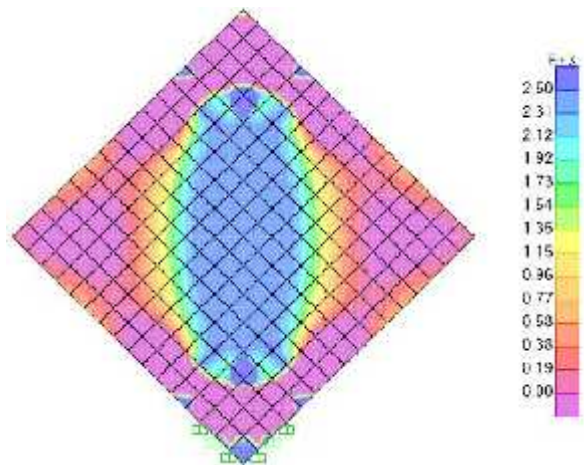


Figure 3.28(b) Crack pattern observed in FEM analysis in SAP 2000

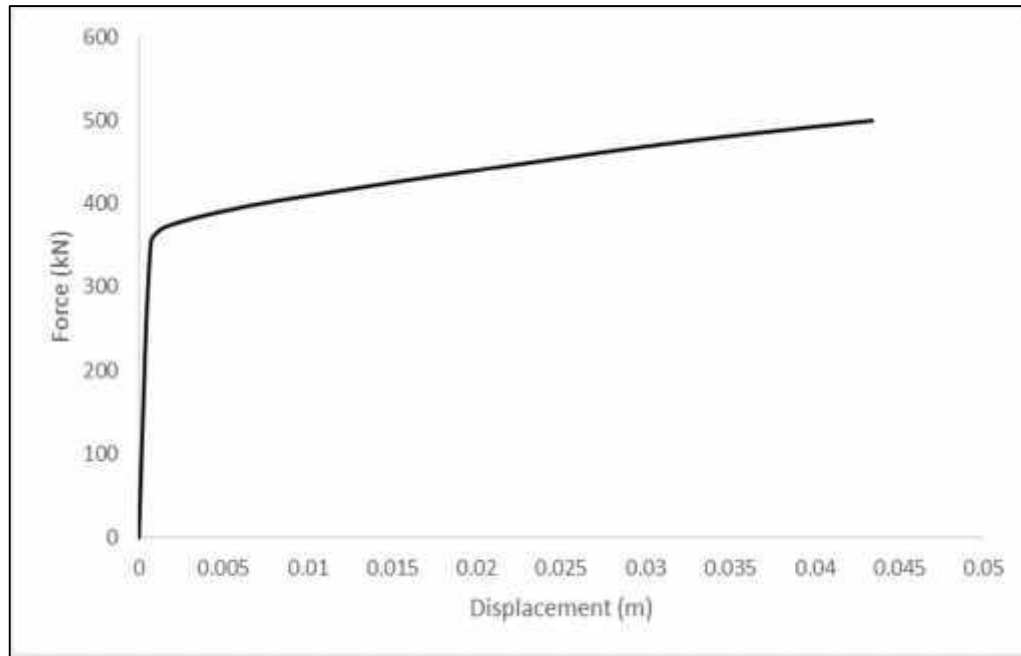


Figure 3.29 Load-displacement curve from simulation of diagonal compression test obtained from SAP 2000

In ABAQUS, finite element simulation of the in-plane shear test of the EPS core panels was performed by modelling the diagonal compression test using the solid 8-noded hexahedral elements. Concrete, expanded polystyrene and welded steel wire mesh were modelled in different layers and the interaction between them were modelled using the ‘tie constraint’ available in ABAQUS, which ensures perfect bond between the layers. By applying the tie constraint, it is ensured that all the connected nodes undergo equal displacements under the application of external load/displacement. The expanded polystyrene core and the two layers of sprayed concrete were modelled using solid 8-noded linear hexahedral element (C3D8) and the welded wire mesh reinforcement was modelled using the 2-noded linear truss element (T3D2). The welded wire mesh reinforcement was embedded inside the concrete layer.



The material behaviour of concrete was modelled using the “concrete damage plasticity” model available in ABAQUS. The grade of concrete used in the study was M25 having characteristic strength (IS 456 200) f_{ck} of 25 MPa. The density of concrete used was 2400 kg/m³ and the value of Poisson’s ratio used in the analysis was 0.2. For concrete, the modulus of elasticity considered was 5000 f_{ck} as given by IS: 456 (2000). The stress-strain curves used for concrete in compression (Desayi and Krishnan, 1964, Hu et al. 2004) and tension (Vecchio 1990) are given in the Figures 3.30 and 3.31, respectively.

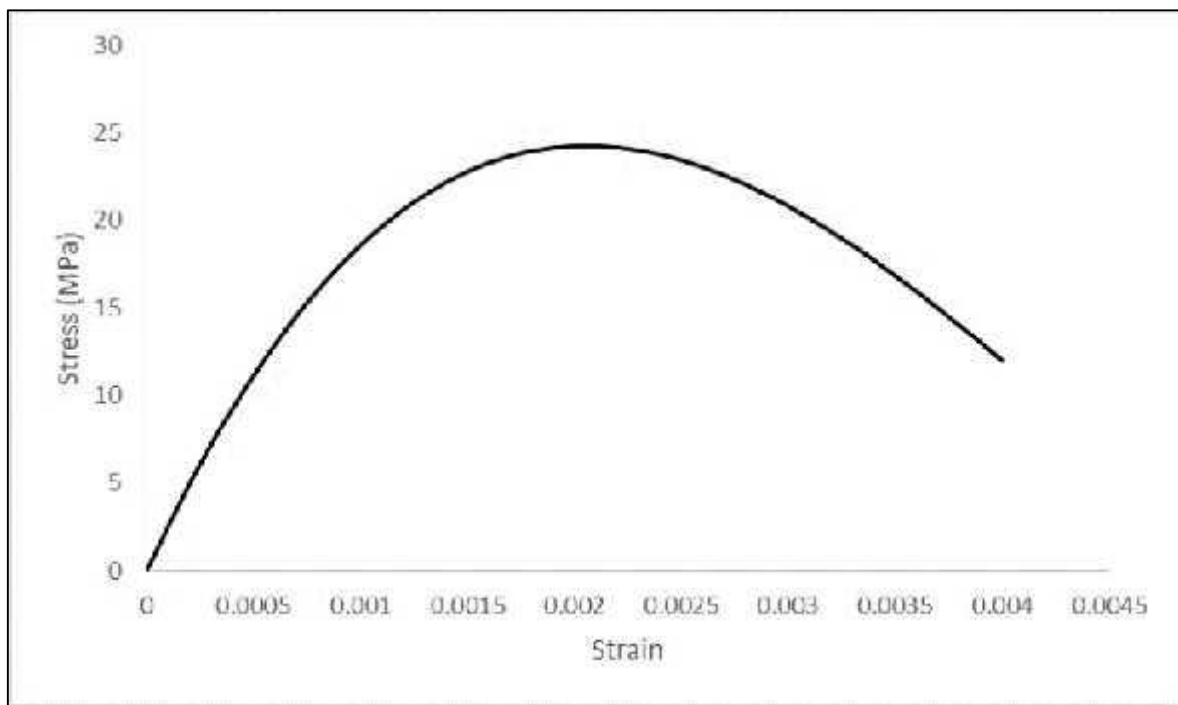


Figure 3.30 Stress-strain curve of concrete in compression

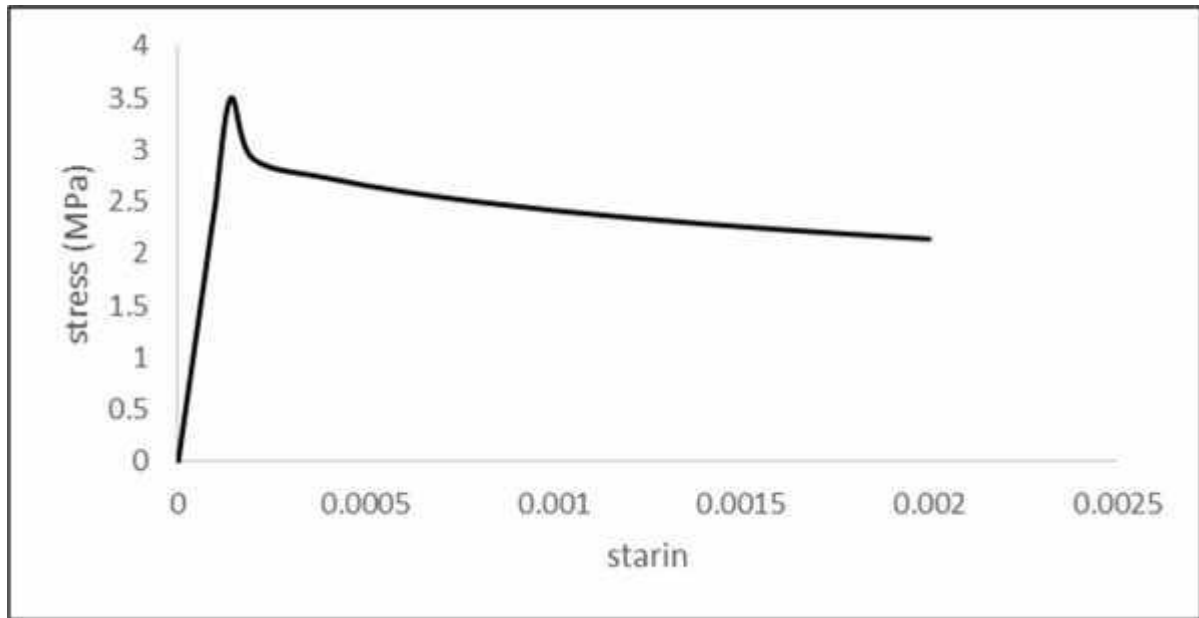


Figure 3.31 Stress-strain curve of concrete in tension

The post yield compression and tension behaviour of concrete was modelled from the above curves in the same manner as used by Jankowiak and Lodygowsky (2005). The yield stress is considered to be almost 0.33 times peak stress in compression and 0.7 times peak stress in tension. The post yield compression and tension curves of concrete are given in Figures 3.32 and 3.33. The compression and tension damage curves for concrete have also been developed using the same procedure as given by Jankowiak and Lodygowsky (2005). The curves for compression and tension damage of concrete are given in the Figures 3.34 and 3.35. The other parameters for concrete damage plasticity model have also been taken from Jankowiak and Lodygowsky (2005). The values of various parameters used in the CDP model are given in the Table 3.2.

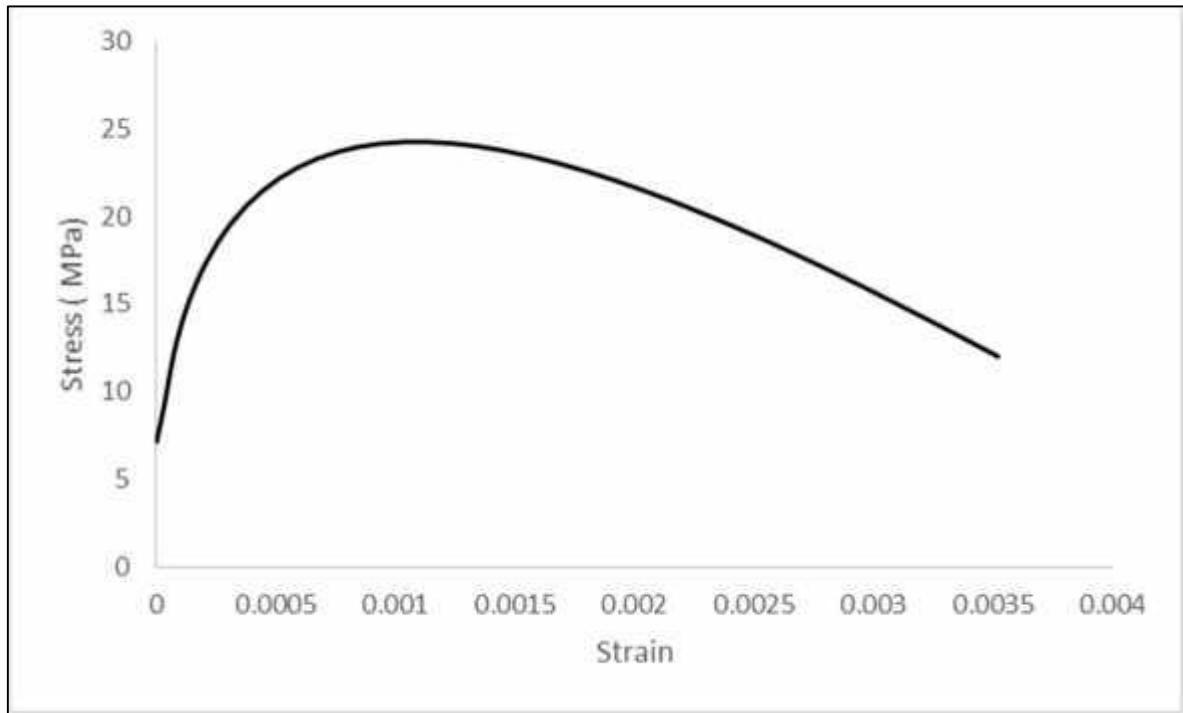


Figure 3.32 Inelastic stress-strain curve of concrete in compression

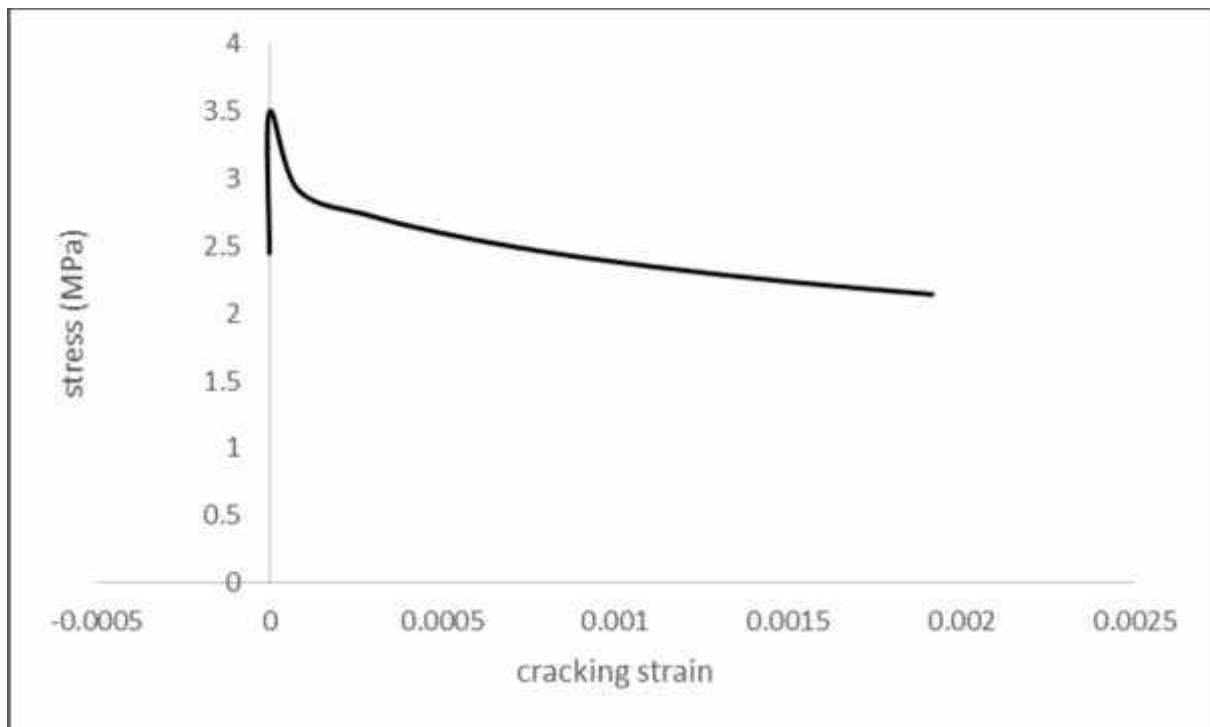


Figure 3.33 Inelastic stress-strain curve of concrete in tension

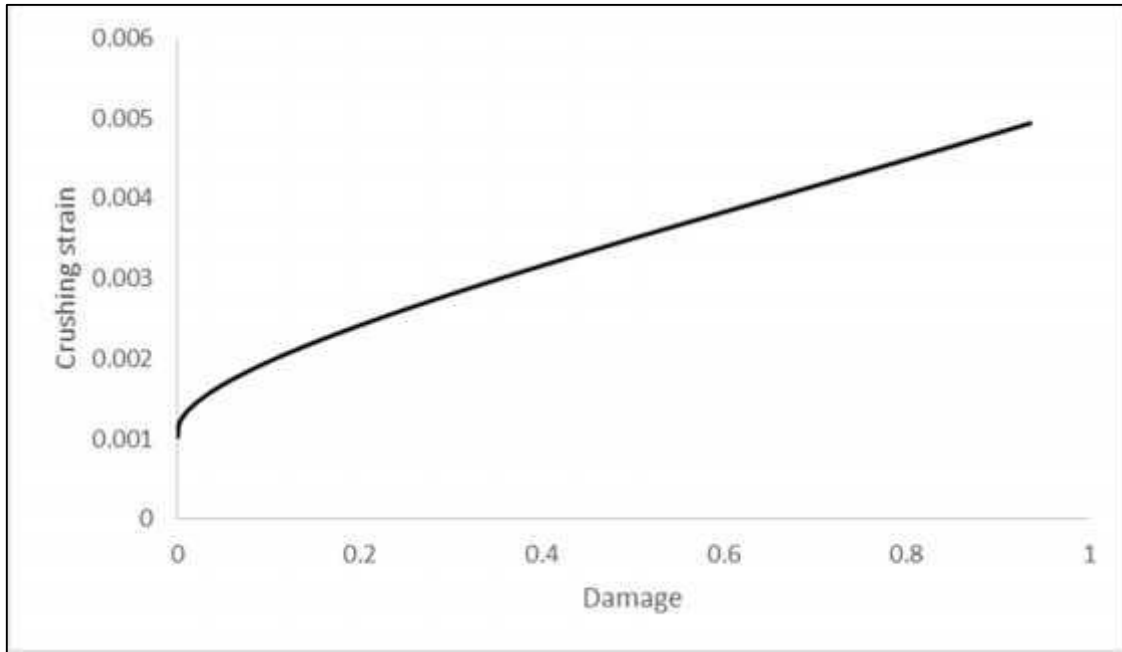


Figure 3.34 Compression damage of concrete

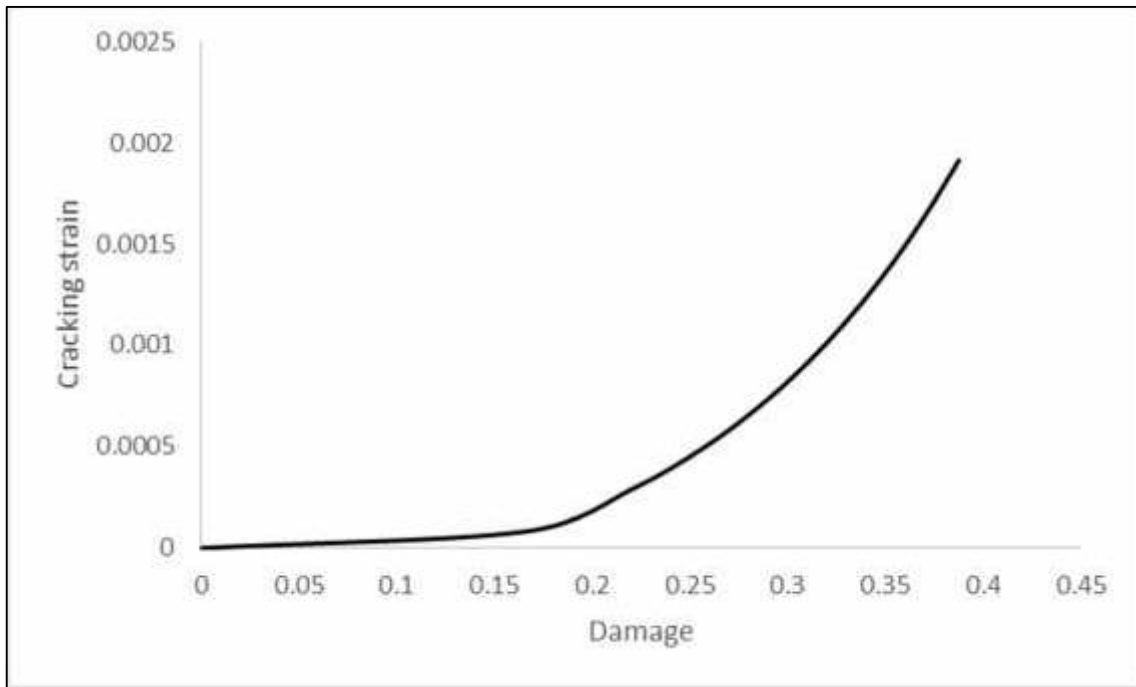


Figure 3.35 Tension damage of concrete



Table 3.2 Parameters used for concrete damage plasticity model

Material	Elastic Modulus (MPa)	Poisson's ratio	Dilation angle	Eccentricity	f_{bo}/f_{co}	k	Viscosity Parameter
Concrete	25000	0.19	38	0.1	1.12	0.67	0

The unit weight of welded wire mesh is considered to be 7850 kg/m^3 . The tensile yield strength of welded wire mesh is considered to be 850 MPa and its elastic modulus is considered as 127 MPa as given by Kadam (2015). The stress-strain curve used for welded wire mesh is given in the Figure 3.36. The expanded polystyrene core is modelled as an elastic material with density as 15 kg/m^3 and its modulus of elasticity is considered to be 25 MPa. Figure 3.37 to Figure 3.40 show the modelling of EPS panels in ABAQUS. The load-displacement curve obtained from the analysis is shown in the Figure 3.41. It is observed that vertical tensile cracks occur in the specimen due to applied load and the boundary condition. The crack pattern obtained from the analysis matches with the crack patterns observed in the experiments performed.

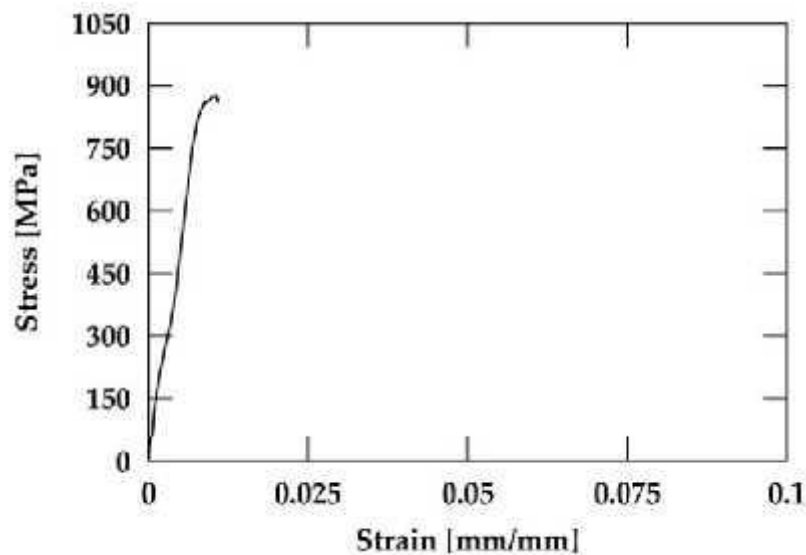


Figure 3.36 Stress-strain curve of welded wire mesh (Source: Kadam, 2015)



Figure 3.37 Model showing the three components of the EPS core panel

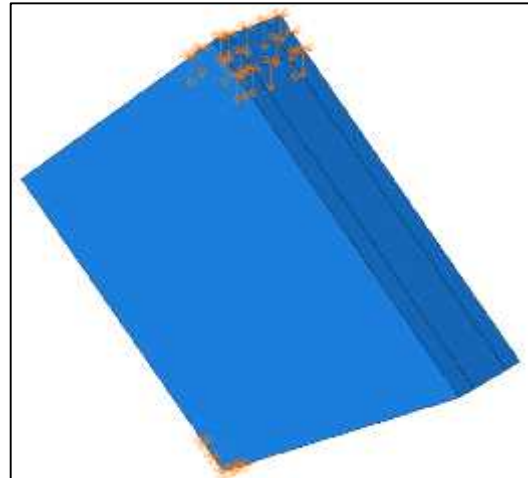


Figure 3.38 Details of loading applied and boundary conditions

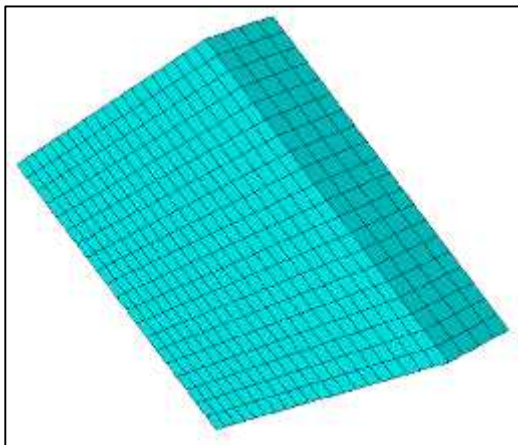


Figure 3.39 Details of finite element mesh

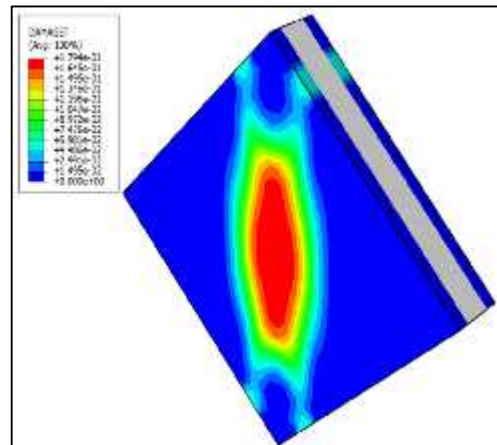


Figure 3.40 Crack pattern obtained from analysis

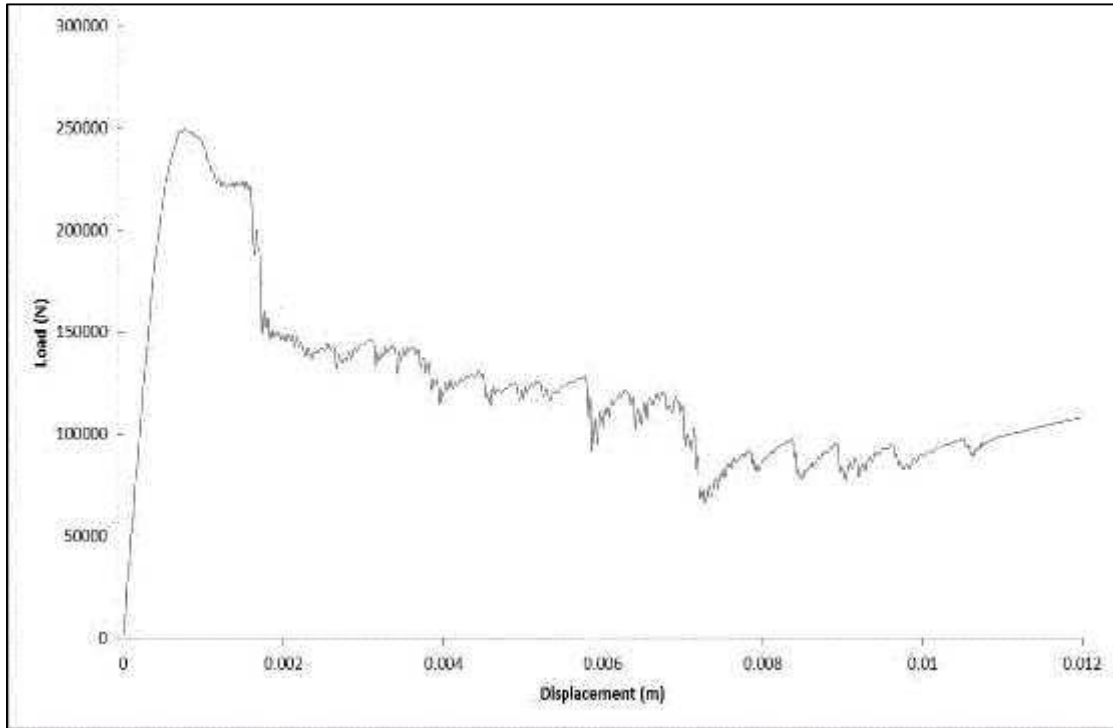


Figure 3.41 Load-displacement curve obtained from nonlinear FE analysis in ABAQUS

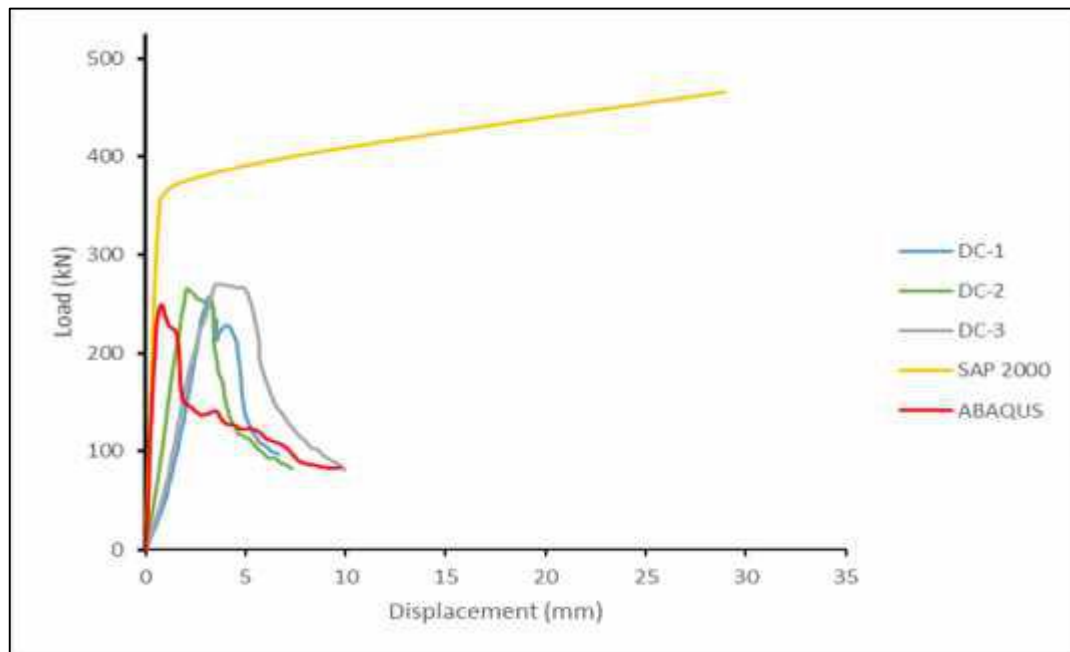


Figure 3.42 Comparative study of numerical analysis and experimental results



Comparison of load-displacement curves of three samples tested experimentally and those obtained numerically using layered shell elements in SAP and nonlinear 3D elements in ABAQUS, is shown in Figure 3.42. It is observed that the results of the finite element modelling done using solid 8-noded hexahedral element in ABAQUS are closer to those of the experimental investigations, while the results of the finite element modelling done in SAP 2000 using layered shell element is quite different. The value of peak diagonal load resisted by the panels obtained by modelling in ABAQUS is equal to 250 kN which is close to the value obtained from the testing of the three specimens. However, the stiffness (slope of the load-displacement curve) from the numerical analysis is much higher than the experimental results. This may be due to the local crushing of the concrete near the top shoe, resulting in higher apparent displacement in the experiment.

To compare with these results, the shear force capacity of the panels is also computed by the formulation given in IS:456 (2000), EC8 and EC2, considering it as a reinforced concrete section with thickness equal to 70 mm (neglecting the thickness of the EPS core). The diagonal force carrying capacity of the section as computed by IS: 456 (2000) method is 242.5 kN and as computed by EC8 and EC2 is 251.4kN , which is close to the values obtained from finite element modelling in ABAQUS and from the experiments performed. The maximum deflection obtained from ABAQUS also matches with that obtained from the experiment. However, the modelling in SAP 2000 using layered shell element overestimates the maximum load carrying capacity of the panels by almost two times and also predicts wrong ultimate displacement value.

3.2.2 Flexure test

To examine the bending behaviour of the EPS panels due to out-of-plane loading, four-point flexural test was performed on the EPS core panels. Size of specimens was 1200mm x 600mm x 150mm. 100mm wide edge beams, were provided on edges normal to the span (along width). The total thickness of the specimen of 150 mm consists of 80 mm EPS at the core and 35 mm concrete layer on each face. The effective span of the panels is 1.1 metres, as the roller supports are provided at a distance of 5 cm from the edges. Expanded

polystyrene core, wire mesh and sprayed concrete are of same specification as used in diagonal compression test. In edge beam 4-#8mm longitudinal bars with rectangular rings of 6mm dia. @ 270mm/c along with #8mm U- shape bars of 300mm length at a spacing of 270mm c/c were provided. Schematic diagram of specimen and flexural test is shown in Figure 3.43.

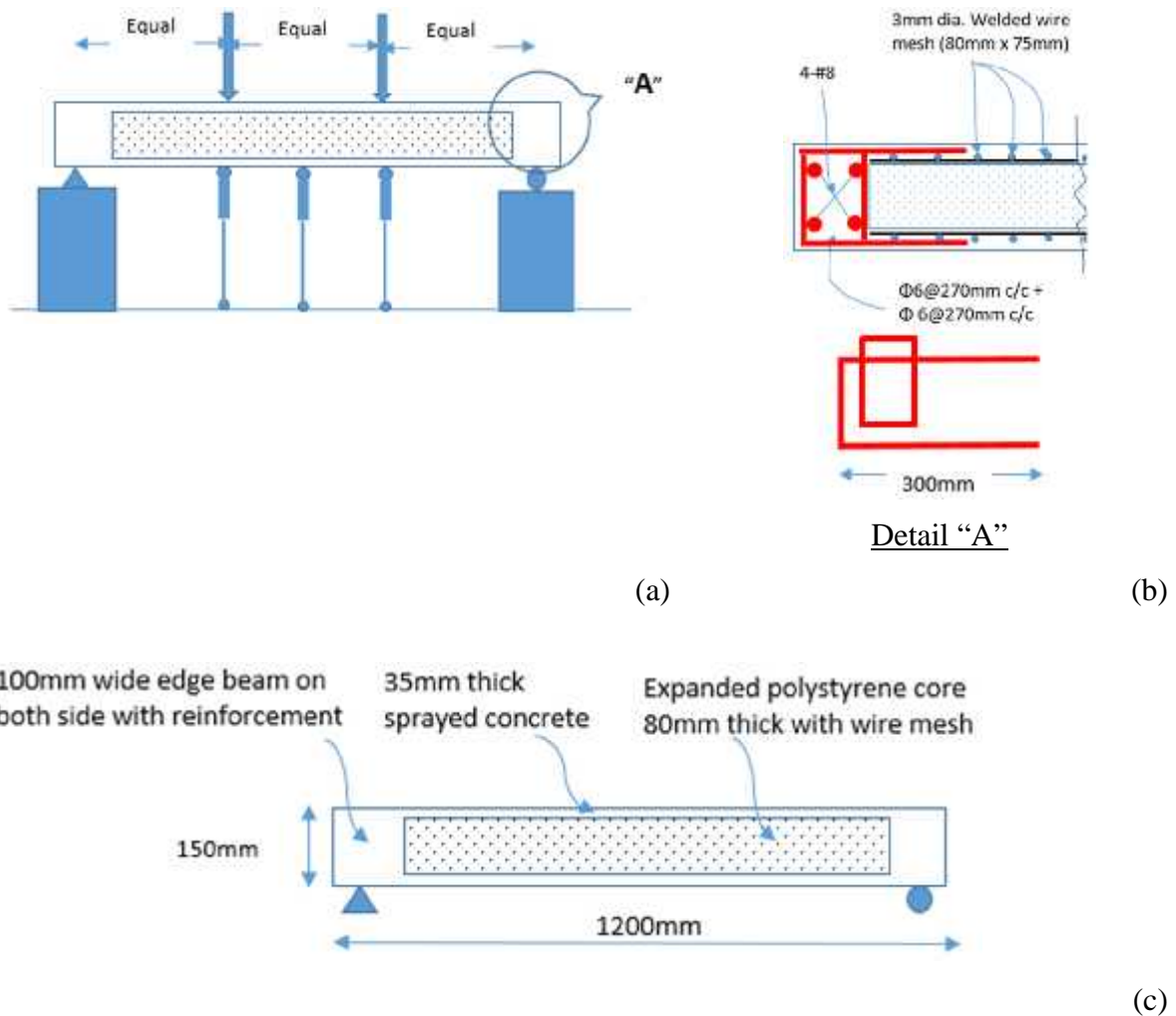


Figure 3.43 Schematic diagram of flexural test: (a) Test setup; (b) Reinforcement details of specimen; and (c) Cross section of specimen



Preparation of mortar mix and spraying of mortar was done using the same equipment as for the diagonal compression test described earlier, e.g. concrete mixer spray gun and air compressor. Figures 3.44 to 3.51 show preparing of specimens for flexural test.



Figure 3.44 Fabrication of form for casting of flexural test specimen



Figure 3.45 Finished form for casting

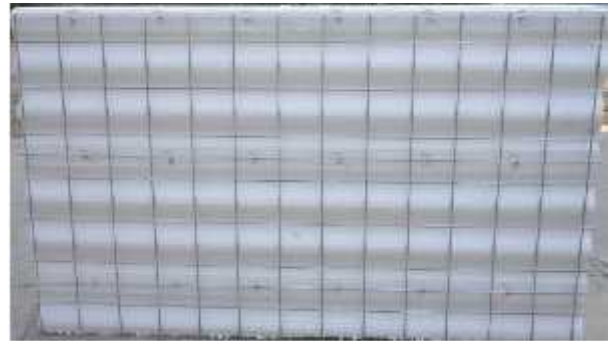


Figure 3.46 EPS panel for flexural test



Figure 3.47 Edge beam reinforcement and beam cage



Figure 3.48 Prepared EPS panel before casting specimen

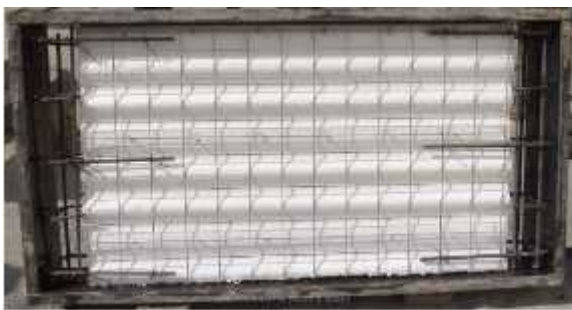




Figure 3.49 Construction of EPS panel for flexural test



Figure 3.50 Casting of edge beam



Figure 3.51 Prepared specimen for flexural test

Three specimens were prepared for flexural strength test. Displacement controlled loading was applied on the panels at two lines parallel to and equidistant from the supports. Linear variable differential transducers (LVDTs) were installed at the bottom of the mid-span and also under the line of load application. Flexure test set up and loading is shown in Figure 3.52. The rate of loading used for the test was 0.2 mm per minute. The load versus mid-span displacement curves of the three specimens are given in the Figure 3.53. The maximum load resisted by the specimen ranged from 30 to 40 kN. It was observed that the peak load was reached when the concrete cracked due to tension at the bottom at mid-span and also under the lines of load application. All the three samples showed similar behaviour. It was also observed that after the maximum load was reached, the load-deflection curves became flat, and de-bonding failure between concrete and steel was observed. The tensile cracks at the bottom developed under the mid-span and also under the line of load application as shown in Figure 3.54. The middle one-third portion of the specimen was subjected to maximum bending moment and thus the cracks occurred in this portion at the bottom due to development of maximum tension in concrete there. Theoretically the ultimate moment capacity of section in non-composite and fully composite case have been calculated as per method suggested by Benayoune, et al., (2008). The ultimate moment capacity in case of non-composite section is 1.36 kN-m and in case of fully composite section is 5.165 kN-m. The average experimental ultimate moment capacity is 6.416 kN-m. The difference in theoretical and experimental values are due to ignoring the contribution of reinforcement in compression.



Figure 3.52 Test setup and loading arrangement for flexural strength test

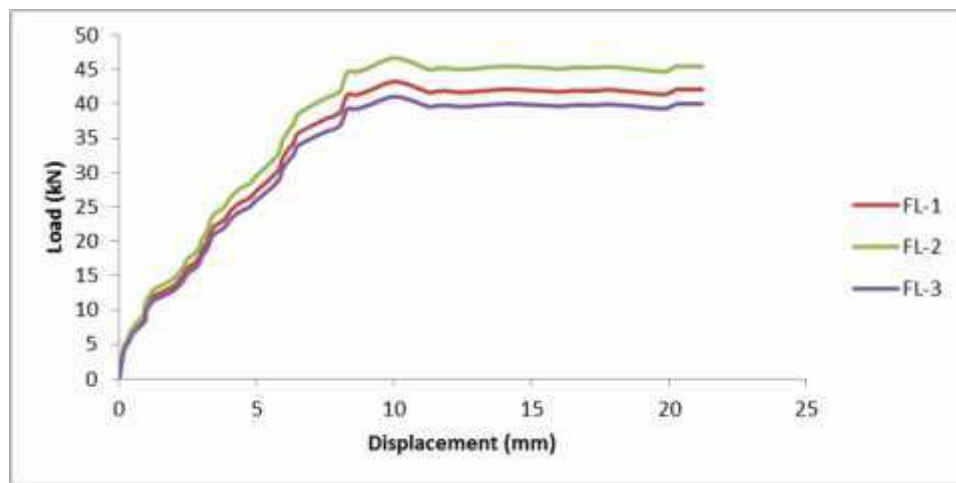


Figure 3.53 Load-displacement curves of flexural test for specimens FL-1 to FL-3



Figure 3.54 Cracks at the mid-span and along the line of application of load



To study the out-of-plane behaviour of the EPS core panels, numerical simulation of flexure test was performed using both SAP2000 and ABAQUS software. Identical specimens were modelled in both software as tested in the laboratory. Finite element model of the panels was developed using layered shell elements in SAP 2000. The properties of the constituent layers are the same as those used for modelling of diagonal compression test. Displacement controlled line loads were applied at one-third length from either side and increased till failure. The details of the model developed, loading applied and boundary conditions are shown in Figure 3.55. The deflected shape observed under the applied loading conditions is given in Figure 3.56. The load versus mid-span displacement obtained from the analysis is given in Figure 3.57.

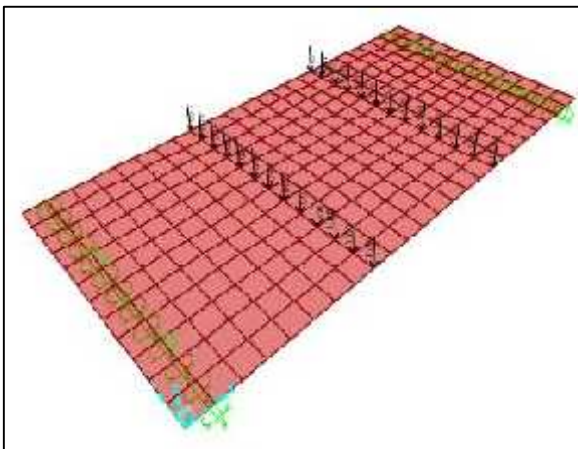


Figure 3.55 Loading, boundary conditions for flexure test in SAP 2000

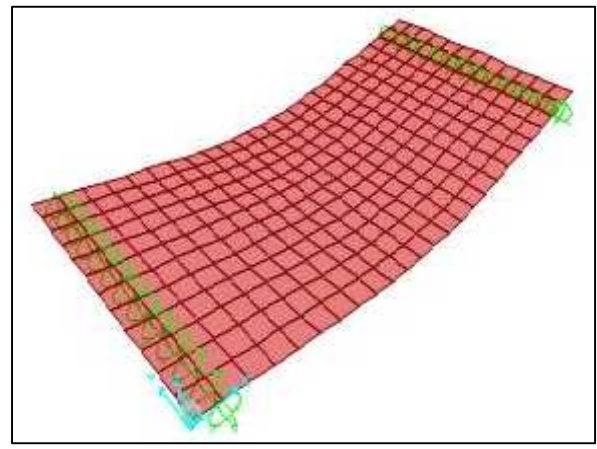


Figure 3.56 Deflected shape due to flexure loading in SAP 2000

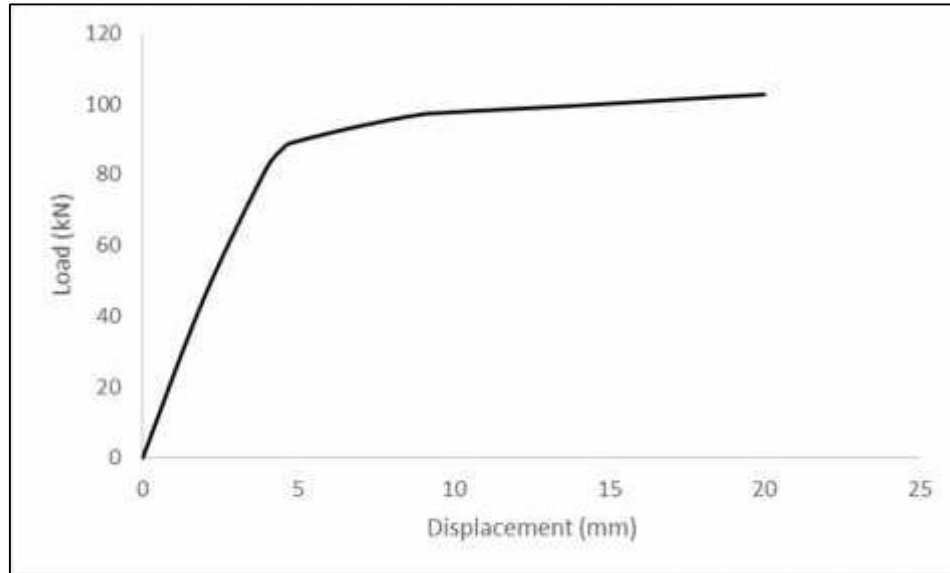


Figure 3.57 Load-displacement curve obtained for simulation of flexure test in SAP 2000

Finite element model of the panels was also developed using ABAQUS. Modelling was done similar to the modelling of diagonal compression test. The model was developed comprising of expanded polystyrene core, the two layers of concrete cover and the welded wire mesh connected by ties are shown in the Figure 3.58. The finite element mesh, and the loading and boundary conditions applied on the model are shown in Figures 3.59 and 3.60, respectively. The deflected shape of the model with tension damage is shown in Figure 3.61 and 3.62. The load versus the mid-span displacement is shown in Figure 3.63.

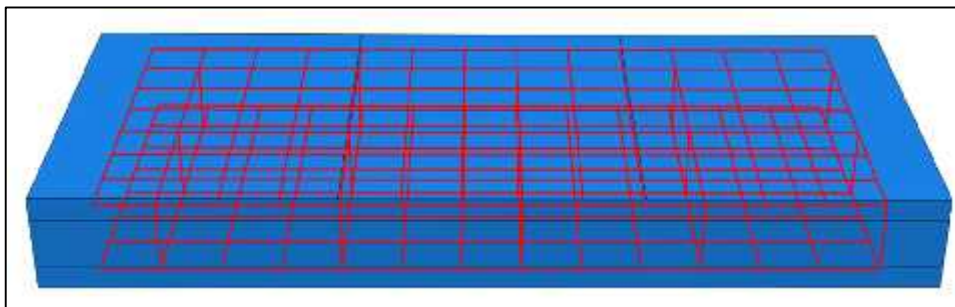


Figure 3.58 Diagram showing components of the FE model developed in ABAQUS for simulation of flexure test

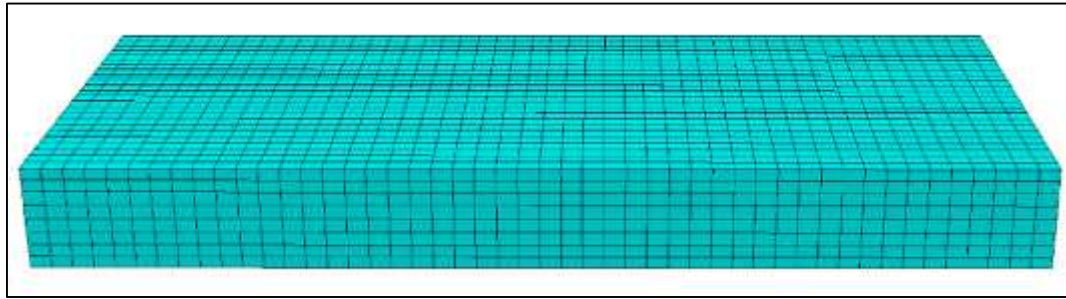


Figure 3.59 Finite element mesh for simulation of flexure test

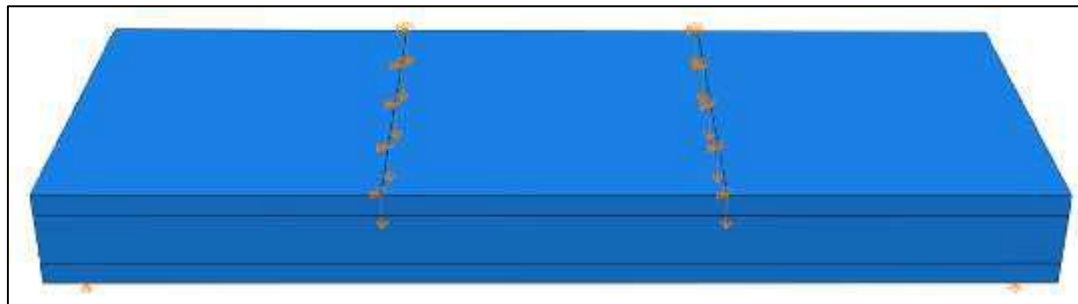


Figure 3.60 Loading and boundary conditions applied for flexure test

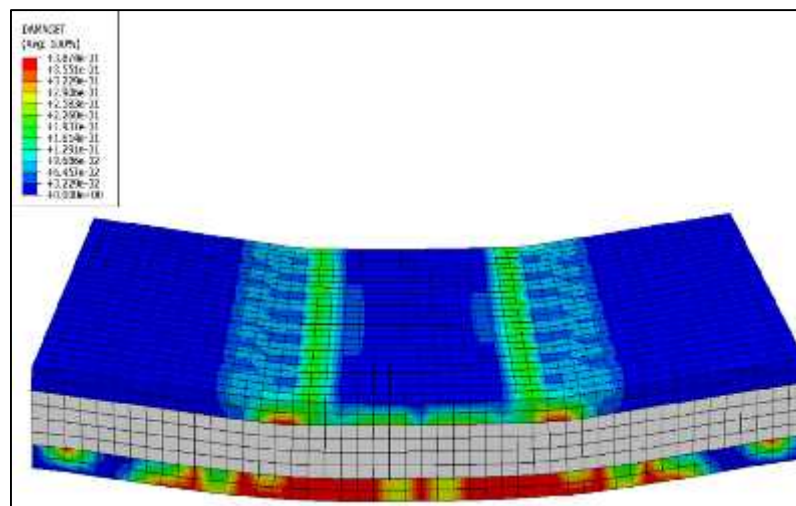


Figure 3.61 Deflected shape of the panel showing tension damage

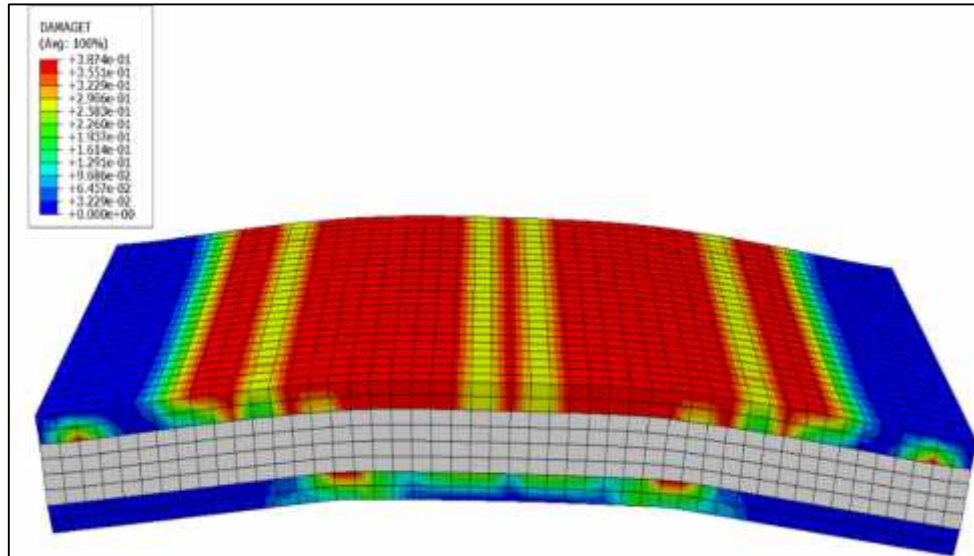


Figure 3.62 Deflected shape, upside down condition to show the tension damage at the bottom

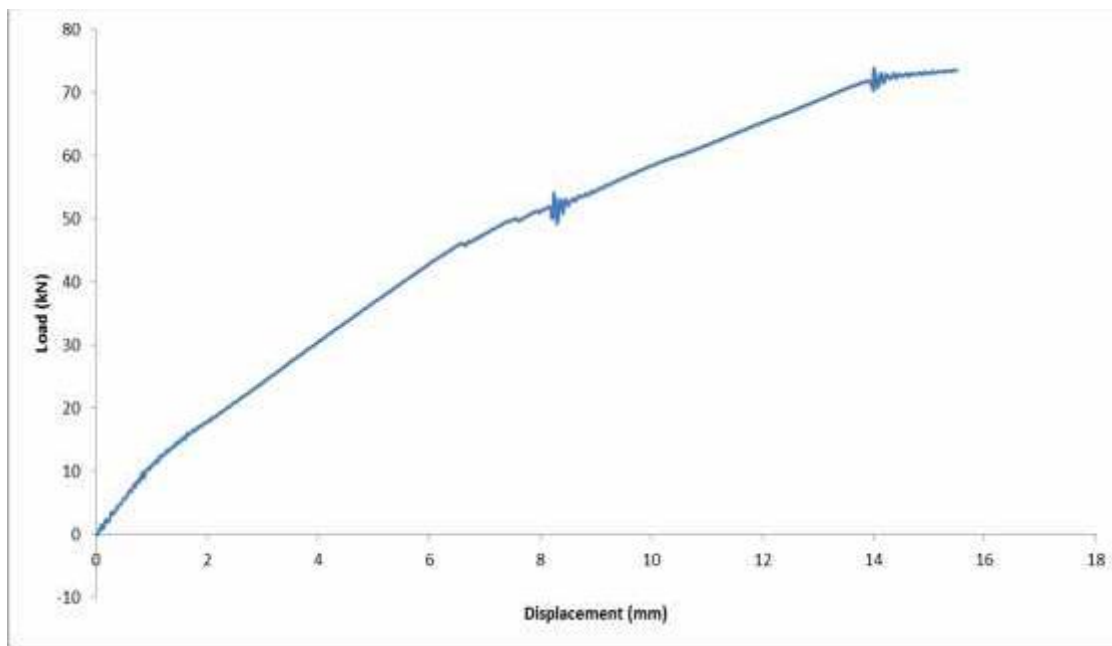


Figure 3.63 Load-displacement curve of four-point loading test as developed in ABAQUS

The load versus central displacement curves of the three specimen tested experimentally and those obtained from modelling in ABAQUS and SAP 2000 are plotted together for



comparison in Figure 3.64. It was observed that the initial portion of the finite element analysis in ABAQUS matches with the experimental curves, but after the tensile failure of concrete, de-bonding occurs in the tested specimen and thus, the latter part of the curves does not match as de-bonding failure has not been considered in the finite element model. The load-displacement curve of the finite element model shows significant strain hardening after the tensile failure of concrete as the steel has not yielded yet and the panel still has the load-carrying capacity. The curve becomes flat after the steel yields and continues till the ultimate strain is reached. However, it has been observed that the results of modelling using layered shell element in SAP 2000 show very high value of stiffness and strength in comparison to the experimental results. The maximum load carrying capacity obtained from modelling in SAP 2000 using layered shell element is almost 2.5 times of that obtained from the experiment.

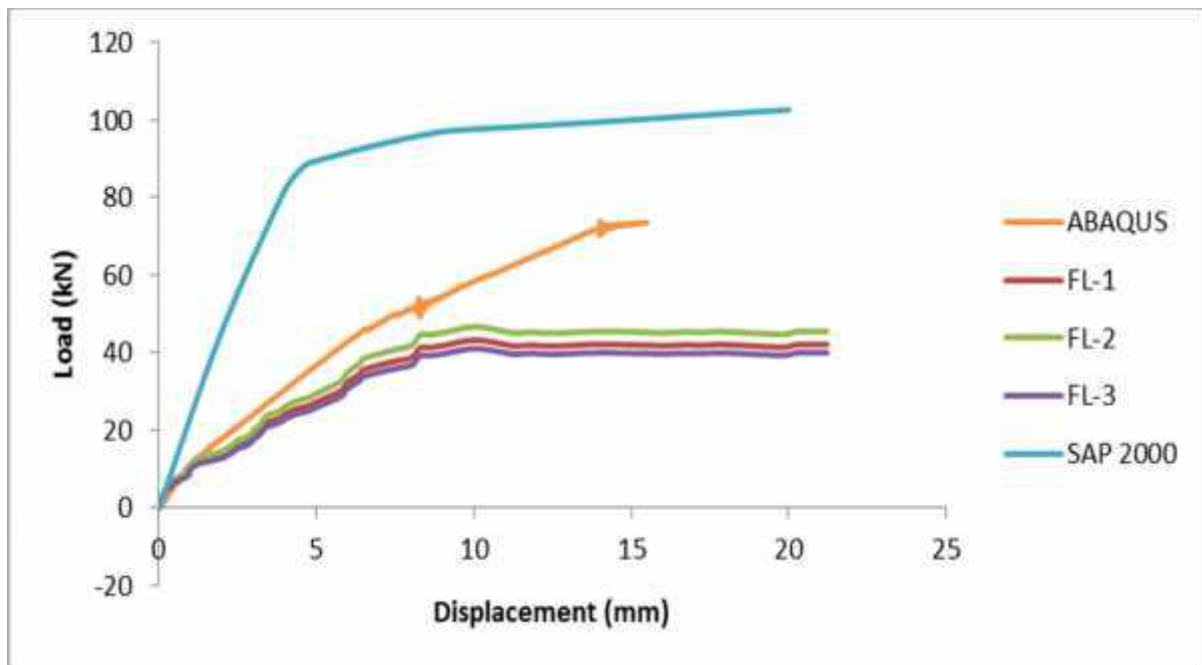


Figure 3.64 Load versus displacement curves obtained from experiment and finite element analysis



This page intentionally left blank.

CHAPTER 4

Seismic Analysis of A Sandwich Wall Panel Building

4.1 Introduction

To evaluate the seismic performance of buildings constructed from sandwich wall panels, a G+3 building built in Sonipat, Haryana, India is studied. Finite element model of the building was developed as per architectural drawings using SAP 2000 Nonlinear software (CSI, 2010). Linear and nonlinear pushover analysis was performed. Stresses in walls due to gravity and lateral load were also calculated using pier analysis and compared with results obtained from linear analysis.

4.2 Building specifications

The G+3 building constructed using the expanded polystyrene sandwich (EPS) core panels, has the following specifications:

- 1) The dimensions of the building are 14.36m (long along y-direction), 12m width (along x-direction) and 13.05m high (along z-direction) with 3m storey height.
- 2) The walls are made of sandwich panels, total 220 mm thick (100 mm thick EPS core, sandwiched between two layers of concrete, each 60 mm thick). The thickness of the concrete layer in the considered building is higher than the normally recommended thickness of 35 mm by the manufacturer. The increased thickness was provided by the designer, apparently from fire endurance requirements.
- 3) The slabs are made of sandwich panels, total 240 mm thick (160 mm thick EPS core, sandwiched between two layers of concrete, upper concrete layer thickness being 50mm and bottom concrete layer thickness being 30mm).
- 4) The superstructure rests on the plinth beams which are 300mm x750mm in size; and the plinth beams rest on columns which have different dimensions: 300mm x



450mm, 300mm x 1015mm, 300mm x 550mm, 300mm x 650mm, 300mm x 900mm, 300mm x 300mm and 300mm x 230mm.

- 5) The panels used for walls and slabs both have welded steel wire-mesh on both the faces close to the interfaces of concrete and expanded polystyrene. The wire-mesh has 3mm diameter and spacing of 80 mm in the horizontal direction and 75mm in the vertical direction. The wire-meshes on the two sides of the EPS panel are also interconnected by connector bars of 3mm diameter.
- 6) The nonlinear analysis presented later in this chapter, shows that the foundation columns yield before the yielding of walls and govern the nonlinear response of the building. Therefore, to study the performance of EPS core panel walls, another case study with the same building, assumed to be founded on a raft has also been considered.

4.3 Material specification

The following material specifications, as available in the building drawings, have been considered in the analytical modelling:

- 1) M-25 grade concrete is used for RCC work and shotcreting (gunnitting) of the panels.
- 2) 3 mm diameter steel wire-mesh having yield strength, f_y equal to 700 MPa is used for the wall panels, and steel having yield strength, $f_y = 500$ MPa is used for the RCC works in foundation.
- 3) Expanded polystyrene sheet of 100 mm thickness is used for the walls.
- 4) Expanded polystyrene sheet of 160 mm thickness is used for the slabs.



4.4 Finite element modelling

The finite element model of the building is developed in SAP 2000, Nonlinear according to architectural drawings. Figure 4.1 shows the plan of the building and Figure 4.2 shows the isometric view of the developed FE model. The walls are modelled using shell elements 120 mm thick, considering the total thickness of the two outer layers of concrete, only. The polystyrene layer is ignored, as it has insignificant contribution in the strength and stiffness of the walls. The floor slabs are also modelled as shell elements ignoring polystyrene layer. Openings in the structure are modelled as per the door and window schedule. Edge constraints are applied to the modelled shells to ensure compatibility of deformations.

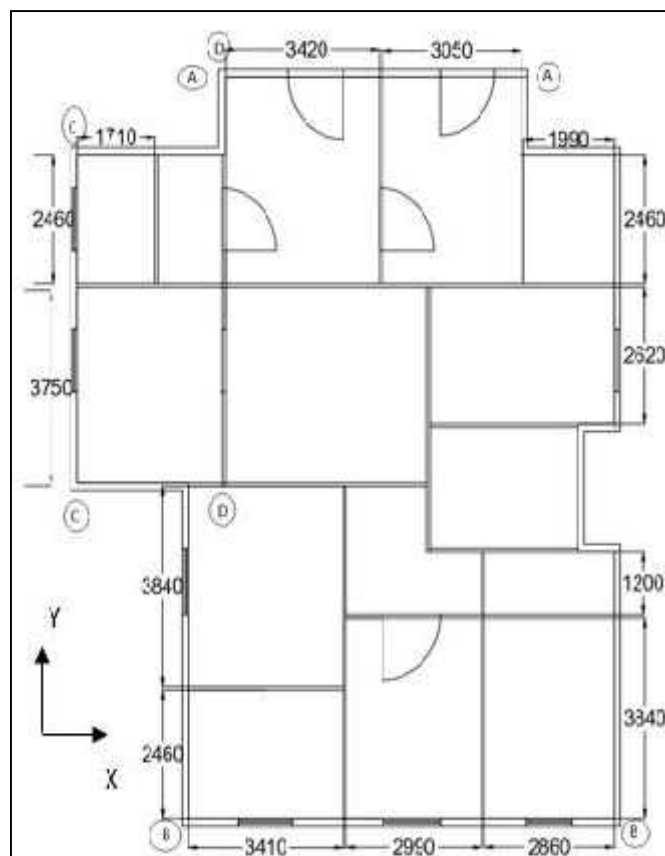


Figure 4.1 Plan of the building (all dimensions are in millimetres)

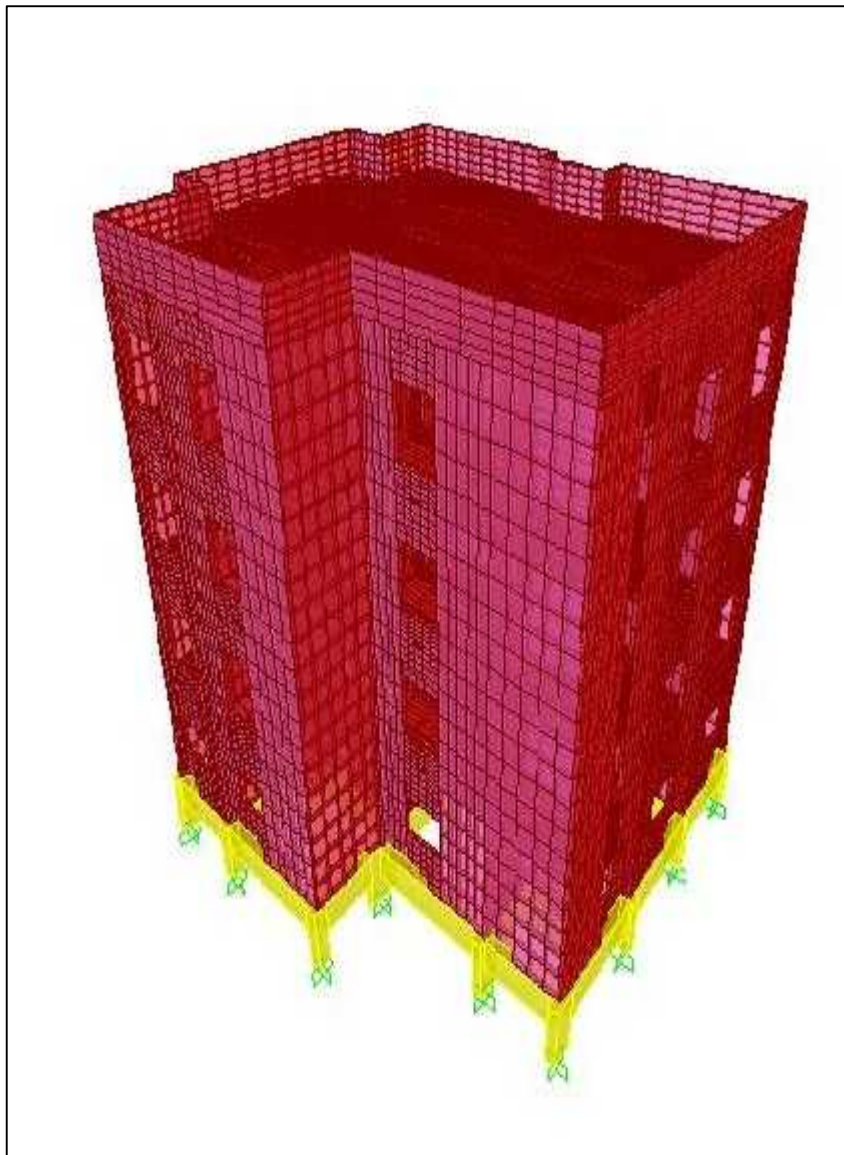


Figure 4.2 Isometric view of the model developed in SAP 2000

The base of the foundation columns is assumed to be fixed. Live loads on the building floors and roof are considered as per IS 875 part 2. Earthquake loads are applied on the model as per IS 1893 (Part 1):2002 and the model is subjected to various load combinations as per IS 1893 (Part 1):2002.



4.5 Pier analysis

Pier analysis is a simplified method of analysis of load bearing wall structures under the combined action of gravity and seismic forces. The details of the analysis method are available in Drysdale et al. (1999). The procedure is based on the following assumptions:

- 1) In-plane and out-of-plane behaviour of walls is considered independently.
- 2) The in-plane behaviour of walls is simulated by an assemblage of piers (i.e. the vertical members consisting of the wall between door and window openings, and below and above the doors and windows).
- 3) The spandrels (i.e. the horizontal members connecting different piers) are assumed to be rigid.
- 4) The end conditions of piers are assumed to be either fixed or free, depending on the restraint expected to be provided by the foundation and the walls above. All the piers have been assumed to be fixed at both the ends, except the upper end of the topmost pier of the building, which does not have much restraining force, and has been assumed to be free.
- 5) In out-of-plane action, the walls have been assumed to span vertically between roof/floor slabs.

The in-plane stiffness (R_i) of a pier is a function of aspect ratio of pier (h/L), thickness of pier (t), elastic modulus of concrete (E) and boundary conditions.

The stiffness of a cantilever pier is expressed as given by Equation (4.1).

$$R_i = \frac{E_c t}{4 \left(\frac{h}{L} \right)^3 + 3 \left(\frac{h}{L} \right)} \quad (4.1)$$

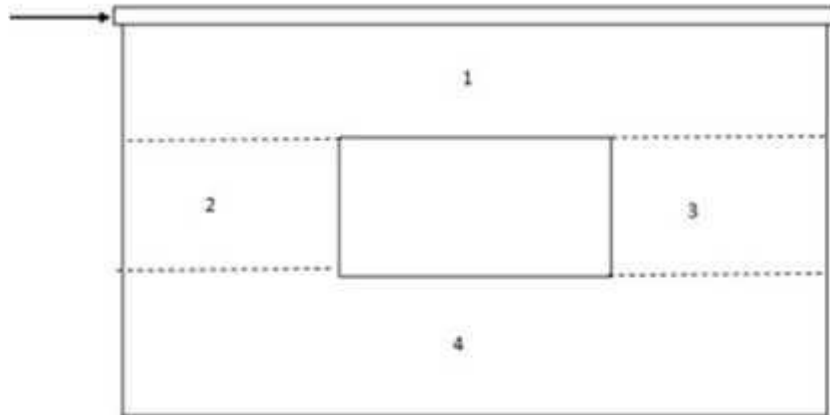


Figure 4.3 Schematic diagram showing different piers in a typical load bearing wall, for use in pier analysis method

Similarly, the stiffness of a fixed end pier is given by Equation (4.2).

$$R_i = \frac{E_c t}{\left(\frac{h}{L}\right)^3 + 3\left(\frac{h}{L}\right)} \quad (4.2)$$

The total stiffness of a wall is obtained from the combination of stiffness of all the piers in parallel and series, following the geometry of the wall.

The total shear force (base shear V_b) in each direction is distributed along the height of the building using the distribution recommended in the Indian seismic code IS 1893-2002 (IS: 1893 Part 1:2002) and the shear in each storey is calculated using Equation (4.4).

$$Q_i = V_b \frac{w_i h_i^2}{\sum w_i h_i^2} \quad (4.3)$$

$$V_i = \sum_{j=1}^n Q_j \quad (4.4)$$



The in-plane forces in individual walls of a storey are estimated from the storey shears obtained from Equation (4.4) and considering the torsion (indicated by design eccentricity, e_d) in the storey. The shear forces in different walls parallel to x and y axes are obtained using Equations (4.5) and (4.6), respectively.

$$F_{xi} = V_{xi} R_{xi} \left(\frac{1}{\sum R_{xi}} + \frac{e_d}{R_s} X_i \right) \quad (4.5)$$

$$F_{yi} = V_{yi} R_{yi} \left(\frac{1}{\sum R_{yi}} + \frac{e_d}{R_s} Y_i \right) \quad (4.6)$$

where,

$$R_s = \sum R_{xi} Y_i^2 + \sum R_{yi} X_i^2 \quad (4.7)$$

and F_{xi} = force in i_{th} wall along x-direction,

F_{yi} = force in i_{th} wall along y-direction,

e_d = design eccentricity as per IS 1893 (Part 1):2002.

R_s = rotational stiffness of storey

R_{xi} = lateral stiffness of i_{th} wall oriented along x-direction

R_{yi} = lateral stiffness of i_{th} wall oriented along y-direction

X_i, Y_i = distances of i_{th} walls from centre of stiffness

Once the shear forces in each wall are known, the shear forces in individual piers are obtained using the procedure described in this Section, earlier. The in-plane bending moment in the piers is obtained from the shear force, as

$$M_k = V_k h_k \quad \text{for cantilever pier, and} \quad (4.8)$$

$$M_k = V_k \frac{h_k}{2} \quad \text{for fixed end piers} \quad (4.9)$$



where, V_k and M_k are the shear force and bending moment, respectively and h_k is the height of the pier.

4.6 Finite element analysis

The response of the building due to combination of gravity and seismic loading has been evaluated using finite element analysis in SAP 2000. At first linear analysis is performed, and the stresses in walls due to most critical load combinations are computed. The axial force, bending moment and shear forces at the critical sections are computed and results are compared with the pier analysis results. The capacity of the members in terms of P-M interaction curves at the critical sections is estimated and checked with the demand obtained from the pier analysis and finite element analysis. Non-linear static pushover analysis is also performed to estimate the performance of the building due to seismic forces.

The FE model of the building has been developed using layered shell elements in SAP 2000. The foundation beams and columns have been modelled as frame elements. The floor and roof slabs are also modelled using layered shell elements. The live load on the floor and roof has been applied according to IS 875, Part 2, consistent with the usage of the building. Analysis for gravity (dead and live) load, free vibration and response spectrum analysis have been carried out. The response spectrum has been considered according to Seismic Zone V and soft soil conditions of IS 1893 (Part 1): 2002. No guidelines are available for selection of response reduction factor, R for such buildings. The present analysis has been performed considering $R=3$. The shear force, bending moment and axial forces at all the critical sections are considered for the different load combinations as per IS 1893 (Part 1): 2002.

It is observed that the total dead load of the considered building is 6270.7 kN, the total live load on floors is 879.8 kN and total live load on roof is 219.9 kN. The base shears in x-



direction and y-direction are 839.9 kN and 806.4 kN respectively. The period of the building in the first mode is observed to be 0.111 seconds and in that in the second mode is 0.108 seconds, indicating a high stiffness to mass ratio, as compared to the RC and masonry buildings of the same height.

4.7 Stresses in walls

The contours of vertical and shear stresses in all the walls, due to the most critical load combinations, are shown in Figure 4.4 to 4.7. It is observed that the maximum stresses due to the applied loads are within the permissible stress limits for concrete according to IS:456 (2000), in all the walls.

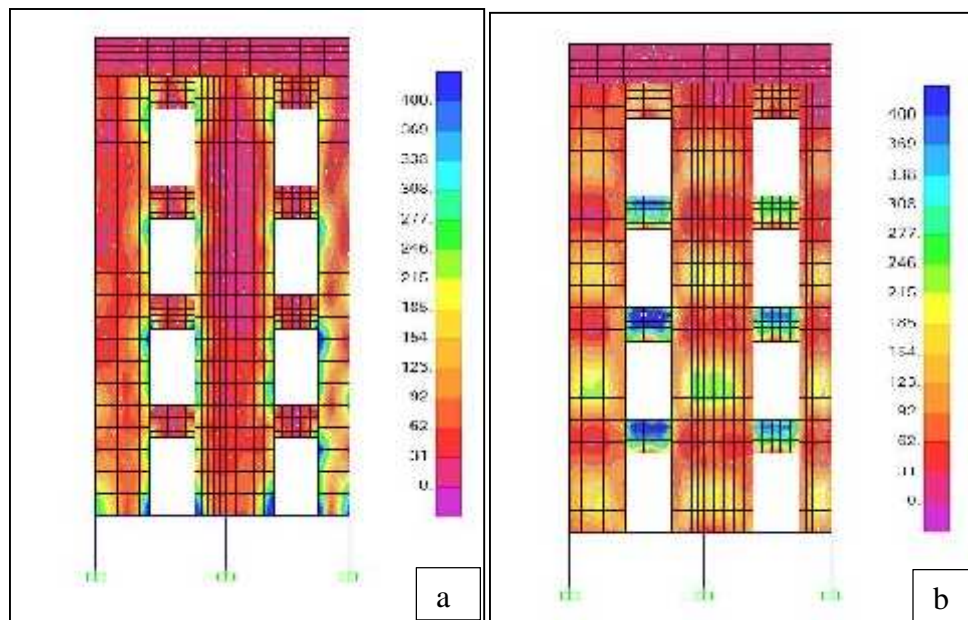


Figure 4.4 Stresses in wall A-A due to the most critical load combination: a) Vertical b) Shear stress (in kN/m^2)

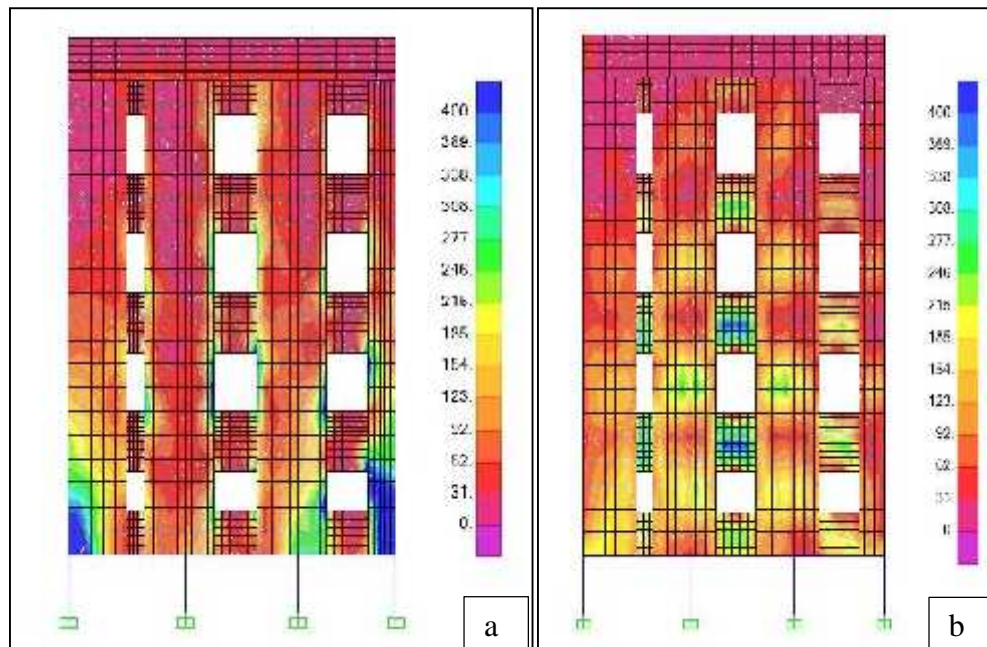


Figure 4.5 Stresses in wall B-B due to the most critical load combination: a) Vertical b) Shear stress (in kN/m^2)

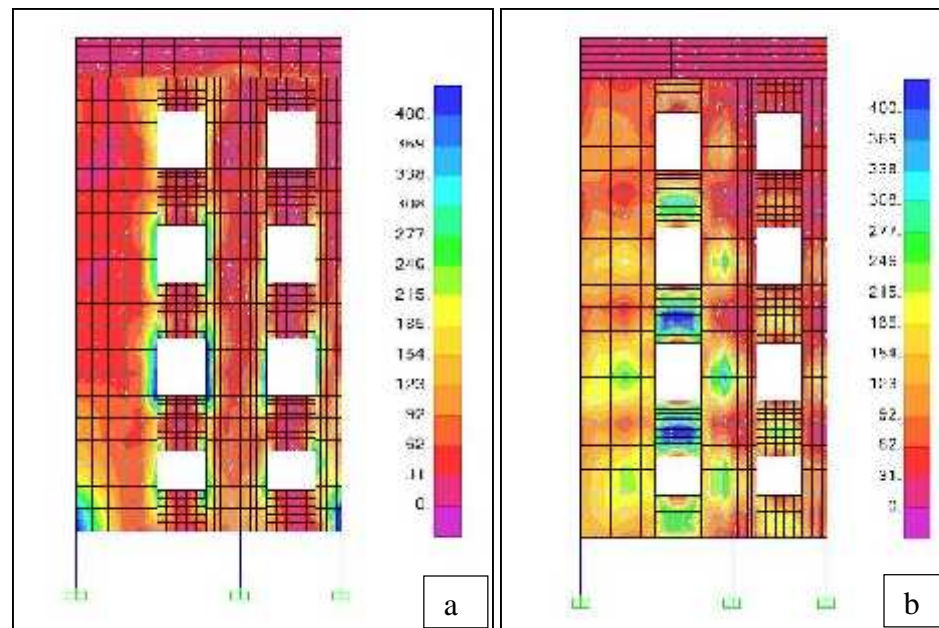


Figure 4.6 Stresses in wall C-C due to the most critical load combination: a) Vertical b) Shear stress (in kN/m^2)

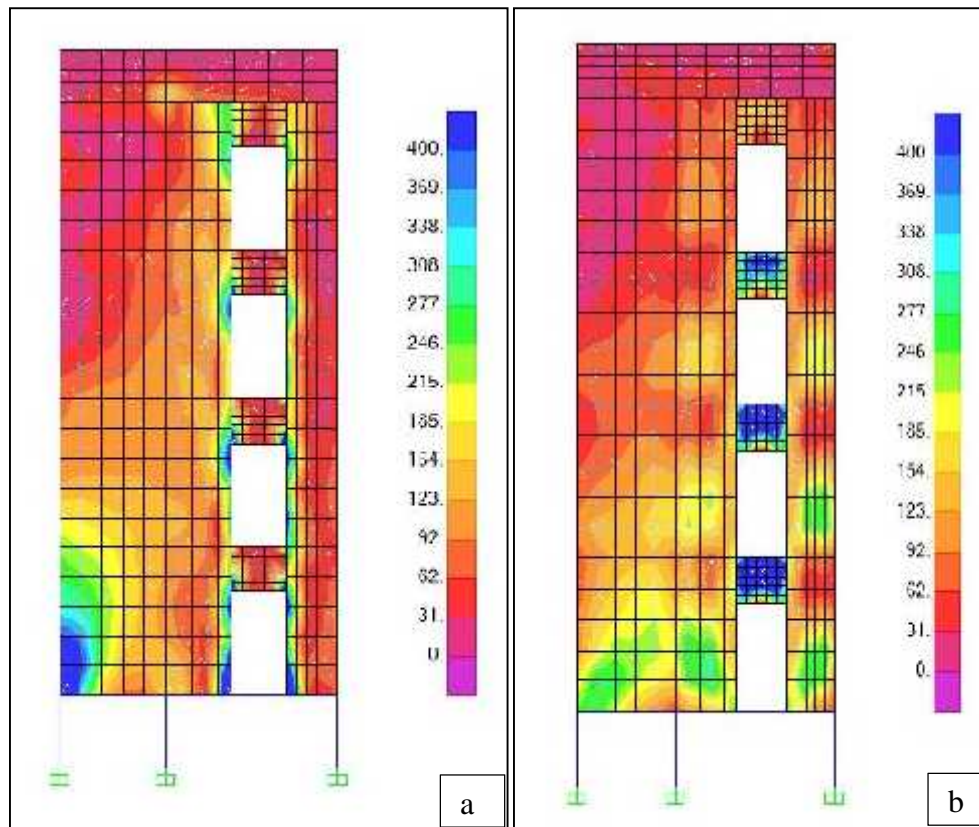


Figure 4.7 Stresses in wall D-D due to the most critical load combination: a) Vertical b) Shear stress (in kN/m^2)

4.8 Comparison of FEA results with pier analysis

Shear forces are computed in all the walls (at each storey) and in the individual piers due to all the load combinations using pier analysis and compared with the finite element analysis results. Table 4.1 shows the calculated shear forces in all the walls at ground storey oriented along the X-direction by both pier analysis and finite element method. For the pier analysis method, values are shown for two cases i.e. considering the effect of torsion and also ignoring the effect of torsion in the building. The wall B-B shown in Figure 4.1 is numbered as WALL-1 and the number is increased along the direction of y-axis, terminating at wall A-A, which is numbered as WALL-9.



Table 4.1 Comparison of pier analysis and finite element analysis (FEA) results for shear force in X-direction walls due to earthquake forces in X-direction

Wall number	Shear force from FEA in SAP 2000 (kN)	Shear force from pier analysis ignoring effect of torsion (kN)	Shear force from pier analysis considering torsion (kN)
WALL 1	117.6	131.2	144.1
WALL 2	46.6	35.3	37.6
WALL 3	48.5	43.4	45.3
WALL 4	71.3	61.1	62.7
WALL 5	134.1	125.4	126.8
WALL 6	43.1	43.9	44.1
WALL 7	186.3	191.1	195.5
WALL 8	62.7	66.9	68.5
WALL 9	66.3	74.2	69.5

The considered building has very low value of eccentricity. Therefore, the values obtained by pier analysis method considering the effect of torsion and ignoring the effect of torsion do not have much difference. It can be observed, that the values of shear forces obtained in the walls by finite element modelling in SAP 2000 are almost same as those obtained by pier analysis method. This resemblance is observed for walls of all the storeys due to all load combinations, in both X and Y directions, thus validating the finite element model.

4.9 Capacity and demand at the critical sections

The axial force and moment carrying capacities of all the critical sections are estimated in terms of P-M interaction curves. The shear force carrying capacity of the sections are calculated using Clause 32.4 of IS 456: 2000. The stress-strain curve of concrete and steel



wire-mesh (considering partial safety factors) used for calculating the capacities of the sections are shown in Figures 4.8 and 4.9, respectively.

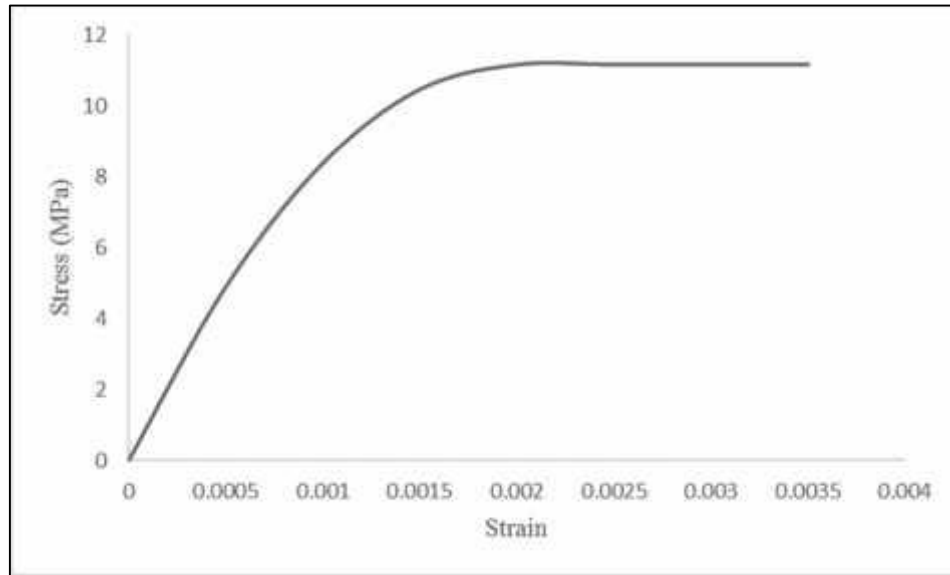


Figure 4.8 Stress-strain curve of concrete used for estimating capacities of sections

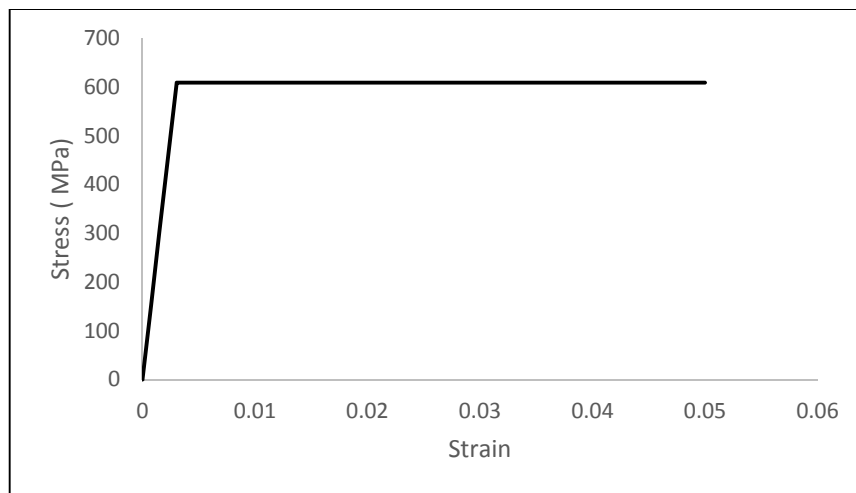


Figure 4.9 Stress-strain curve of steel wire-mesh used for estimating capacities of sections

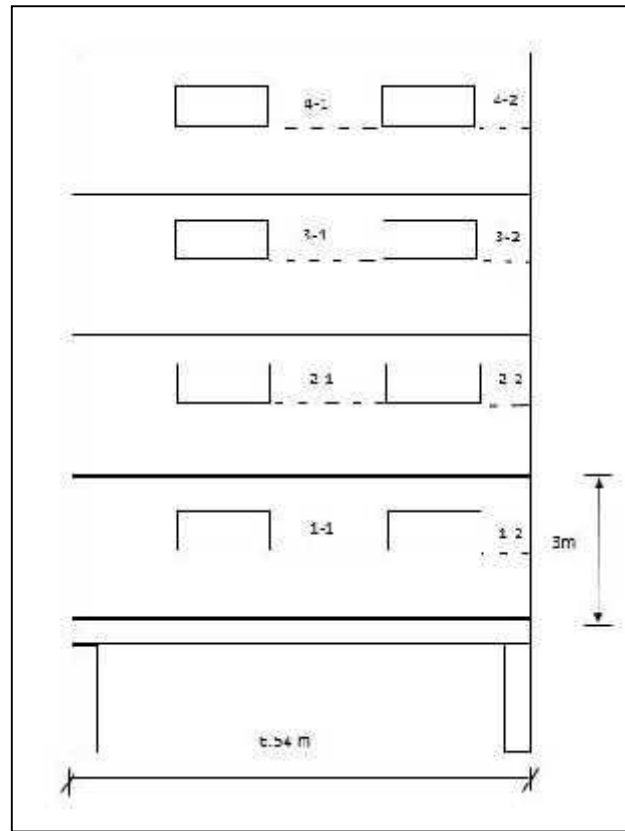


Figure 4.10 Schematic diagram showing the critical section cuts of wall C-C marked in the plan view of the building

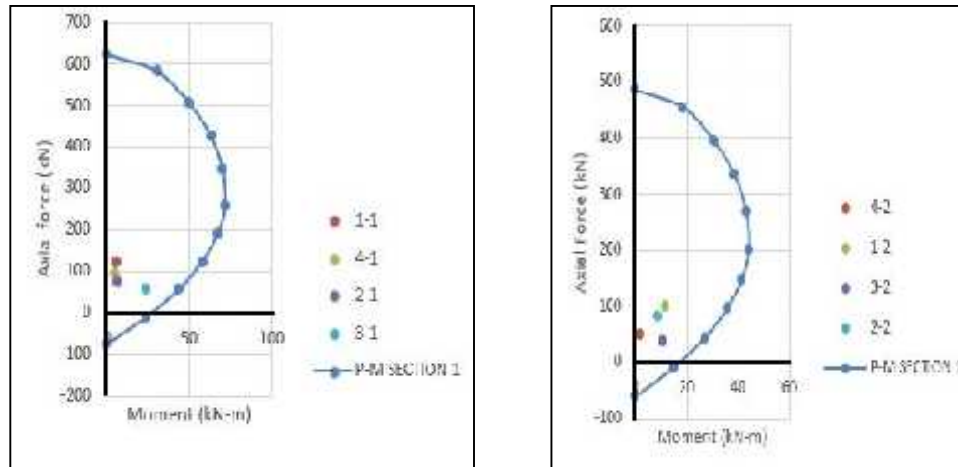


Figure 4.11 P-M interaction curves of a few critical sections showing demand forces



The axial force, bending moment and shear force acting on the critical sections under all the considered load combinations are then compared with the capacity values obtained. The P-M interaction curves and the demand forces of a few sample critical sections are shown in Figure 4.11. In all the cases, it is observed that the load carrying capacity of the sections is greater than the demand on the sections. The P-M interaction curves and the plot of the demand forces on them show that the demand capacity ratio is less than 1 for all the critical sections of the building. Thus, from the results of linear analysis, it can be concluded that the design of the building is adequate to withstand the earthquake forces.

4.10 Non-linear static pushover analysis

The linear analysis presented in the previous Section is based on an assumed value of Response Reduction Factor, R . The assumed value of the response reduction factor is validated by estimating the over-strength and ductility of the structure. To estimate the over-strength and ductility and to understand the behaviour of the structure due to earthquake, non-linear static pushover analysis has been performed using nonlinear layered shell elements in SAP 2000. The non-linear behaviour of the beams and columns in the foundation has been simulated using the lumped plasticity models as per the guidelines of ASCE 41. The pushover analysis has been performed under application of gravity and lateral loads. The lateral load has been applied in both X- and Y- directions, separately and has been continued from the end of the gravity load case which is a combination of dead and live loads. The lateral loads are applied proportional to the fundamental mode in the respective direction. The results of the non-linear static pushover analysis yield the relationship between the lateral base shear and the corresponding roof displacement at successive loading steps.



It was observed from the results of the pushover analysis that most of the lateral lateral deformation occurred in the foundation beams and columns, whereas the superstructure remained almost rigid. The failure also occurred due to failure of the beams and columns, indicating that these are the weaker links in the whole structural system. Therefore, pushover analysis was also performed on the same building with foundation considered as raft. Deflected shapes of the buildings with two types of foundations is compared in Figure 4.12.

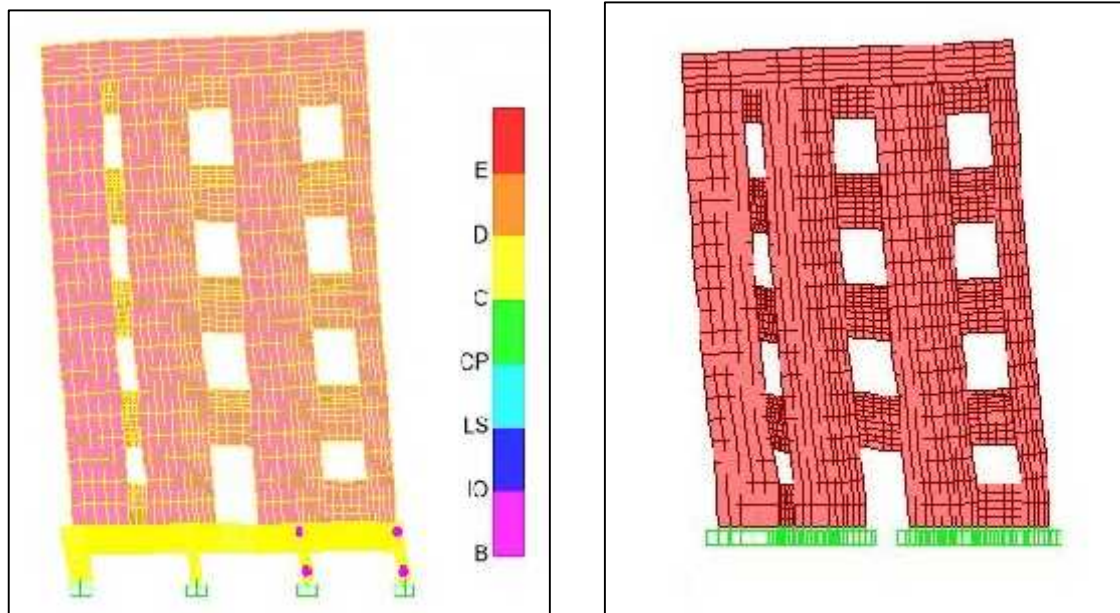


Figure 4.12 Deflected shape of the building with: (a) beam-column foundation; and (b) raft foundation

It is observed that the building behaved as a more rigid structure in case of raft foundation, the period of the building reduced from 0.11 sec to 0.077 sec in first mode. It was also observed that there was increase in the deformation capacity of the building when the beam-column foundation was replaced by raft foundation, as shown in Figures 4.13 to 4.14.

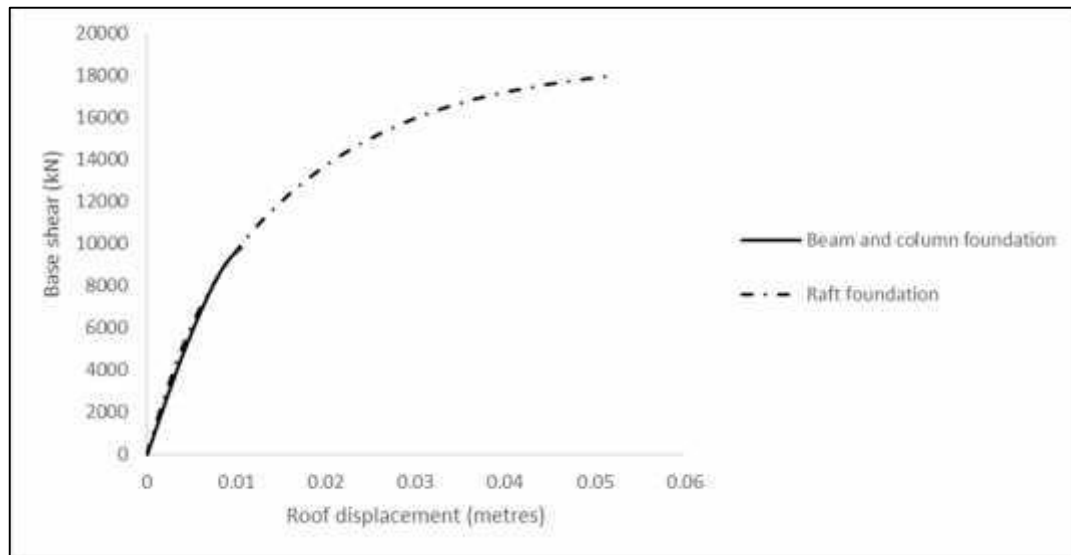


Figure 4.13 Capacity (Pushover) curves of the building in X-direction

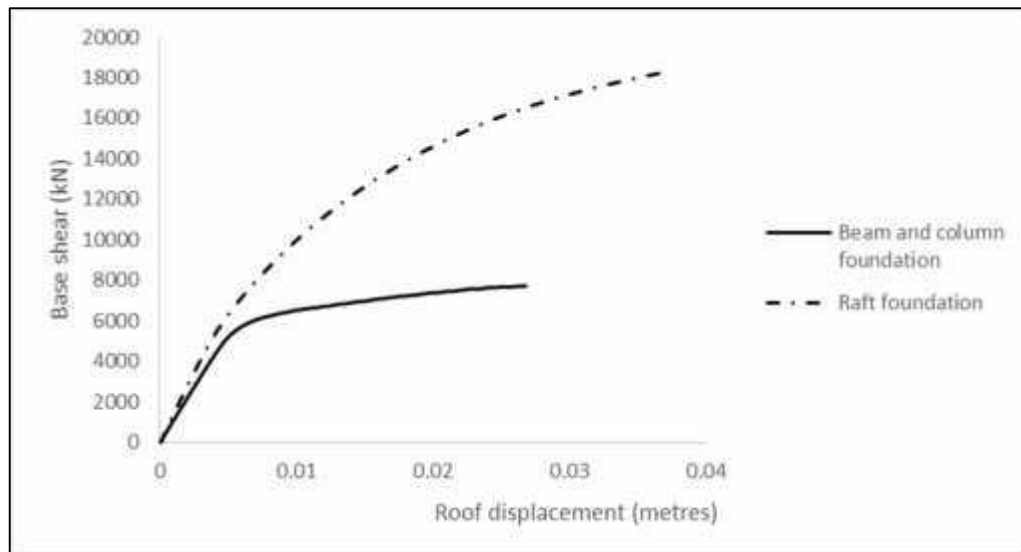


Figure 4.14 Capacity (Pushover) curves of the building in Y-direction



The performance point of the building for Design Basis Earthquake (DBE) and Maximum considered Earthquake (MCE) in both X and Y directions have been estimated using the Displacement Modification Method (DMM) of ASCE 41 and the displacement demand in the two cases is shown in Table 4.2. It can be observed from the Table that the estimated roof drift in case of raft foundation is much lower than that in case of the beam-column foundation. This is due to the fact that there is increase in rigidity for the case with raft foundation in comparison to the building with beam column foundation. Further, the drift demand, in both the cases, is much smaller in comparison with the conventional building systems and is also much lower, even under MCE, than the capacity. This is mainly due to the much reduced seismic weight of the EPS core building, in comparison with the conventional building systems.

Table 4.2 Roof drift (%) at performance points

Loading Direction	Building with Beam Column Foundation			Building with Raft Foundation		
	DBE	MCE	Capacity	DBE	MCE	Capacity
X	0.74	1.38		0.68	1.18	
Y	0.30	0.80		0.24	0.68	

CHAPTER 5

Design Guidelines

5.1 Introduction

In this Chapter guidelines for analysis and design of EPS sandwich wall panel buildings are presented. Requirement of thickness of wythes as per fire rating and durability is also discussed in this Chapter. Before starting of structural design of any structure there is requirement of forces acting in various load resisting elements at critical sections due to action of various loads and their combinations. More accurate analysis can be performed using FEM with the help of software like SAP2000 and ABAQUS or any other available FEM based software to obtain design forces, but as shown in the previous chapter, simpler calculations using ‘Pier Analysis’ also yield fairly good results for gravity and seismic loads. After getting the design forces, the structural elements such as walls, slabs, foundation etc. can be designed for compression, moment and shear, using simple RC design theory with some modifications.

5.2 Design of wall panels for Compression

5.2.1 Pure axial compression in solid panels

Ultimate load carrying capacity of sandwich panel walls under pure axial case may be calculated using Equation 5.1 (ACI 318-89) or 5.2 (Benayoune, 2007). These equations are only applicable when panel behaves fully composite, applied load is in “middle-third” of wall thickness and slenderness ratio is not more than 25.

$$P_u = 0.55W f_{cu} A_c [1 - (kH / 32t)^2] \quad (5.1)$$

$$P_u = 0.4 f_{cu} A_c [1 - (kH / 40t)^2] + 0.67 f_y A_{sc} \quad (5.2)$$



where,

f_{cu} = Characteristic cube strength of concrete

f_y = Tensile strength of steel

P_u = Ultimate axial load

$k = 0.8$, for wall restrained against rotation

Φ = Capacity reduction factor = 0.7

A_{sc} = Total area of steel

A_c = Gross area of wall panel

H = Effective height of wall panel

t = Thickness of the panel section

5.2.2 Axial compression in panels with opening

Load carrying capacity of sandwich panels having openings may be calculated using Equation 5.3 (Saheb and Desayi, 1990). The influence of size and location of the opening(s) is taken into account through the parameter γ .

$$P_{uoc}^c = (k_1 - k_2 \gamma) P_{uc}^c \quad (5.3)$$

$$P_{uc}^c = 0.55 \Phi [A_g f_c' + (f_y - f_c') A_{sv}] [1 - (H/32t)^2] [1.2 - (H/10L)] \quad (5.4)$$

where,

$$\gamma = \frac{A_0}{A} + \frac{a}{L}$$

$$A_0 = L_0 t, \quad A = Lt, \quad a = [(L/2) - \tilde{a}]$$

$$\tilde{a} = [(L^2 t / 2) - L_0 t a_0] / (Lt - L_0 t)$$

P_{uoc}^c = Theoretical ultimate load for panel with opening;



P_{uc}^c = Theoretical ultimate load for panel without opening;

A_g = Gross area of the wall panel section;

A_{sv} = Area of vertical steel in wall section;

L_0 = Length of panel opening ;

f_c' = Cylinder strength of concrete;

f_y = Yield strength of steel;

H, L, t = Height, length and thickness of wall panel;

k_1 & k_2 = Constants;

$k_1 = 1.0027$

$k_2 = 0.779$

a_0 = Distance of the centre of the opening from the left edge of the panel;

a = Distance between centres of panel with and without opening; and

\tilde{a} = Distance of the centre of the panel without opening from the left edge of the panel.

5.3 Axial force-moment interaction

Strength of eccentrically loaded short sandwich panels may be calculated using Equations 5.5 and 5.6, proposed by Benayoune, et al., (2006). These equations are derived using the principles of linearity in strain, strain compatibility and equilibrium as shown in Figure-5.1.

Following assumptions are made:

- a) The two wythes acted in fully composite manner.
- b) Parabolic stress strain curve is replaced by rectangular stress strain curve having depth $(S) = 0.9x$, x is depth of neutral axis
- c) The compressive stress in the extreme compression fiber is $0.45f_{cu}$, and the corresponding ultimate strain $v_{cu} = 0.0035$.
- d) The tensile strength of concrete is neglected.



$$P_u = F_{cc} + F_{sc} - F_s$$

$$P_u = 0.45 f_{cu} BS + f_{sc} A_{sc} - f_s A_s \quad (5.5)$$

$$M_u = P_u e$$

$$M_u = F_{cc} \left(\frac{h}{2} - \frac{S}{2} \right) + F_{sc} \left(\frac{h}{2} - d_1 \right) + F_s \left(\frac{h}{2} - d_2 \right) \quad (5.6)$$

where,

P_u = Ultimate axial load

M_u = Ultimate moment

e = Eccentricity

f_{cu} = Characteristic cube strength of concrete

F_{cc} = Compressive force in concrete

F_{sc} = Compressive force in compressive steel

F_s = Tensile force in steel

f_{sc} = Compressive stress in compressive steel

f_s = Tensile stress in tensile steel

A_{sc} = Total area of steel

A_s = Gross area of wall panel

h = Total thickness of wall panel

S = Depth of equivalent stress block

d_1 = Distance between most compressive fibre to compression steel

d_2 = Distance between most compressive fibre to tension steel

v_{cu} = Ultimate strain in concrete

v_s = Strain in tensile steel

v_{cs} = Strain in compressive steel

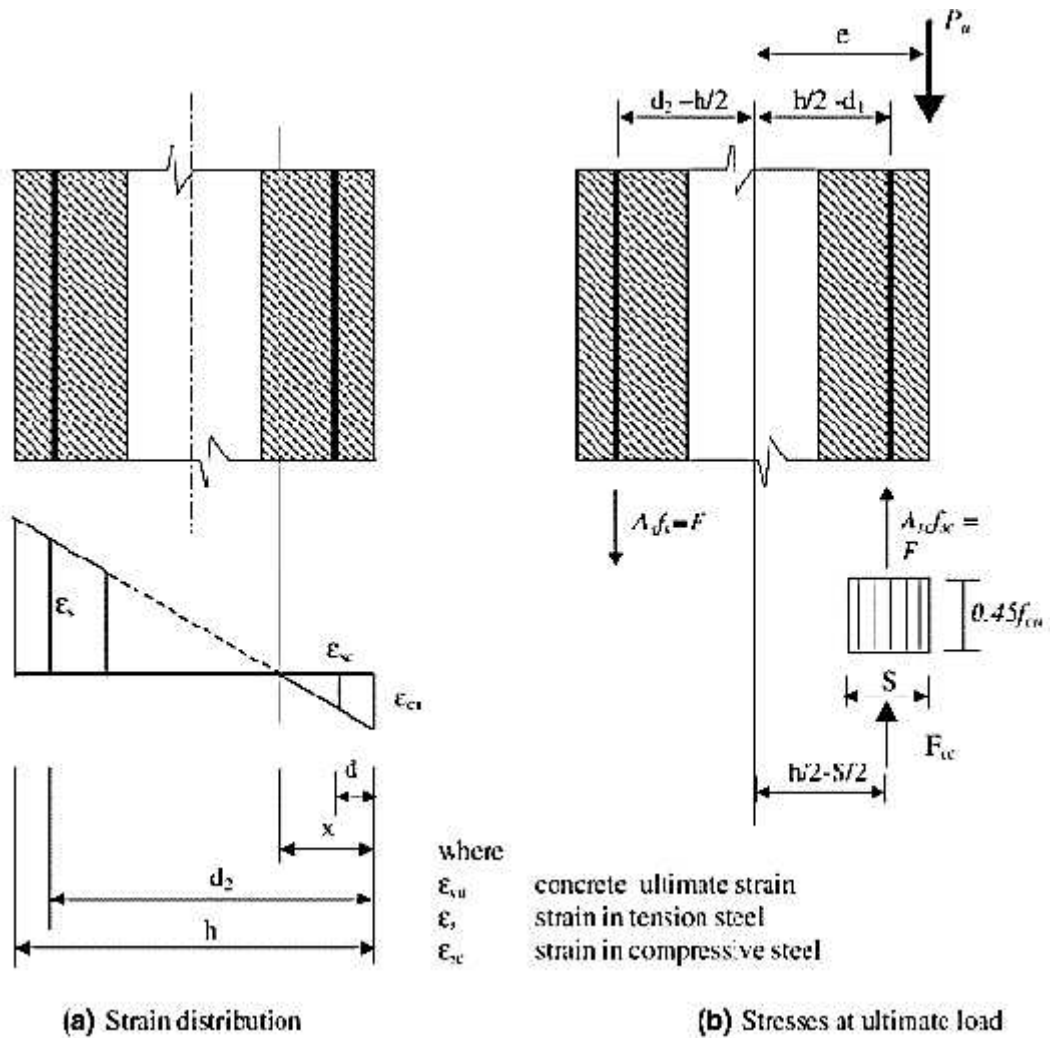


Figure-5.1 Variation of strain and stresses on a composite panel cross-section subjected to eccentric axial loading

The above described method may lead to non-conservative estimates as it assumes fully composite action between the different layers of the composite panel. Benayoune, et al., (2008), and Mohamad, et al., (2014) calculated degree of composite action and ultimate strength, analytically. Benayoune, et al. (2008), suggested that the distribution of stress across the depth, up to linear stage can be used for evaluating degree of composite action.



Ratio of effective moment of inertia (I_e) to Gross moment of inertia (I_g), (assuming full composite action) provides the degree of composite action.

$$I_e = \frac{Mh}{(\uparrow_b - \uparrow_t)} \tag{5.7}$$

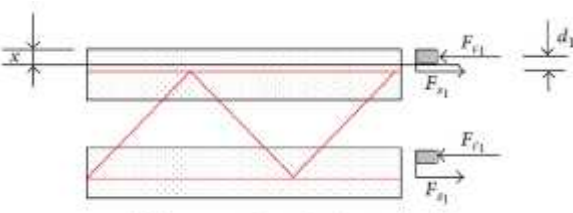
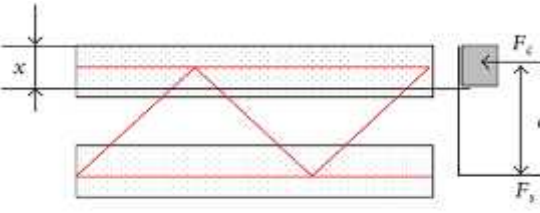
where,

\uparrow_t, \uparrow_b = Stresses at top and bottom;

M = Applied bending moment; and

h = Depth of panel.

Ultimate load resisted by the panel can be determined as follows:

Non Composite action	Composite action
<div style="text-align: center;">  <p>(a) Noncomposite action (1 meter length)</p> </div> <p> $F_{s1} = A_s f_y$, $F_{c1} = 0.85 f_{cu} b s_1$ $F_{s1} = F_{c1}$, $s_1 = F_{s1} / F_{c1}$ F_{s1} = Force in tension reinforcement (non-composite) $M_{u(oneythe)} = F_{s1} \left(d_1 - \frac{s_1}{2} \right)$ $M_u = 2M_{u(oneythe)}$ M_u = Ultimate moment capacity F_{c1} = Comp. force in conc. (non-composite) </p>	<div style="text-align: center;">  <p>(b) Fully composite action (1 meter length)</p> </div> <p> $M_u = T(d - s/2)$ M_u = Ultimate moment capacity F_c = Comp. force in conc. F_s = Force in tension reinforcement $s = 0.9x$, where x is depth of neutral axis </p>



A_s = Area of tension reinforcement b = per meter length of wall section or connector spacing f_y = Yield stress of steel $s_1 = 0.9x$, Depth of neutral axis	
---	--

Upto 3.0m span single sandwich panels can be used for slab and roof of residential buildings, beyond 3.0m span ribbed beam type sandwich panels serve the deflection and strength criteria. Trombetti, et al., (2012b), developed analytical formulation for calculation of bending resistance, axial resistance, shear resistance and their combinations of sandwich panels, on the basis and assumptions of RC theory. These formulation can be applied to large lightly reinforced concrete (LLRCW) walls with spread reinforcement if there is full composite action and shear connectors do not buckle.

Evaluation of Moment resistance M_u for given axial load N of LLRCW

$$\tilde{M}_u = (f_y \dots b y_u) \left(\frac{h}{2} - \frac{y_u}{2} \right) + [f_c b 0.8(h - y_u)](0.1h + 0.4y_u) + A_{s,add} f_{y,d} (h - 2c) \quad (5.8)$$

$$y_u = h \left[\frac{0.8 - \frac{N}{f_c b h}}{0.8 + \frac{f_y \dots}{f_c}} \right] \quad (5.9)$$

where,

f_y = Yield strength of steel

f_c = Compressive strength of concrete

\dots = Geometric ratio of vertical reinforcement



y_u = Position of neutral axis in ultimate condition

ϵ = Normalised axial force

$$\epsilon = \frac{N}{f_c b h}$$

$A_{s,add}$ = Cross sectional area of the additional bars placed at the ends of wall

c = Re-bar cover

5.4 Shear capacity

Shear strength of a sandwich panel may be calculated as per Clauses 40.2 and 40.3 of IS 456:2000. Shear stress due to design shear force acting at the section (τ_v) is to be compared with the nominal shear stress capacity of section (τ_c), shown in Table -5.1. In no case design shear strength be more than maximum shear strength ($\tau_{c,max}$) of section shown in Table- 5.2.

$$\tau_v = \frac{V_u}{b d} \quad (5.10)$$

If design shear stress (τ_v) is more than shear stress capacity of section (τ_c), provide additional shear reinforcement as per design. Shear reinforcement shall be provided to resist shear force equal to

$$V_{us} = V_u - \tau_c b d \quad (5.11)$$

$$V_{us} = \frac{0.87 f_y A_{sv} d}{s_v} \quad (5.12)$$

where,

V_u = Shear force due to design load

b = Length of wall



d = Effective depth

A_{sv} = Area of horizontal shear reinforcement

s_v = Spacing of horizontal shear reinforcement

f_y = Yield strength of steel

Table -5.1 Shear capacity of section without shear reinforcement (τ_c) N/mm² (IS 456, 2000)

$100 \frac{A_s}{bd}$	Concrete Grade					
	M 15	M 20	M 25	M 30	M 35	M 40 and above
(1)	(2)	(3)	(4)	(5)	(6)	(7)
≤ 0.15	0.28	0.28	0.29	0.29	0.29	0.30
0.25	0.35	0.36	0.36	0.37	0.37	0.38
0.50	0.46	0.48	0.49	0.50	0.50	0.51
0.75	0.54	0.56	0.57	0.59	0.59	0.60
1.00	0.60	0.62	0.64	0.66	0.67	0.68
1.25	0.64	0.67	0.70	0.71	0.73	0.74
1.50	0.68	0.72	0.74	0.76	0.78	0.79
1.75	0.71	0.75	0.78	0.80	0.82	0.84
2.00	0.71	0.79	0.82	0.84	0.86	0.88
2.25	0.71	0.81	0.85	0.88	0.90	0.92
2.50	0.71	0.82	0.88	0.91	0.93	0.95
2.75	0.71	0.82	0.90	0.94	0.96	0.98
3.00 and above	0.71	0.82	0.92	0.96	0.99	1.01

Table -5.2 Maximum shear stress at section ($\tau_{c,max}$) N/mm²

Concrete Grade	M 15	M 20	M 25	M 30	M 35	M 40 and above
$\tau_{c,max}$, N/mm ²	2.5	2.8	3.1	3.5	3.7	4.0

Evaluation of ultimate shear strength V_u according to the Eurocode

Ultimate shear strength V_u for a given axial force N in a Lightly Reinforced Concrete Wall (LLRCW), can be obtained using EC8 and EC2 provisions (Trombetti, et al., 2012b). The



shear capacity, V_u is the smaller of shear resistance of horizontal reinforcement and the concrete strut resistance.

Shear horizontal reinforcement resistance (V_u)

$$V_u = \frac{A_{sw}}{s} z f_y (\cot \alpha + \cot \gamma) \sin \gamma \quad (5.13)$$

Concrete strut resistance (V_u)

$$V_u = 0.6 b z f_c \gamma_c (\cot \alpha + \tan \alpha) \quad (5.14)$$

where,

A_{sw} = Area of horizontal shear reinforcement

s = Spacing of horizontal shear

z = Inner lever arm

α = Angle between concrete compression struts and the main tension cord = 22°

γ = Angle between shear reinforcement and the main tension cord = 90°

γ_c = 1 as per EC2

Evaluation of ultimate sliding resistance according to the Eurocode

The shear stress at interface of two concrete members casted in different times must satisfy the following expressions according to the EC8 and EC2 provisions:

$$\epsilon_{Edi} \leq \epsilon_{Rdi} \leq 0.5 \epsilon_c \quad (5.15)$$

$$\epsilon_{Edi} = S V_E / (z b) \quad (5.16)$$

$$\epsilon_{Rdi} = c f_{ctd} + \sim \left(\frac{N_E}{A_c} + \dots f_y \right) \quad (5.17)$$



$$\epsilon = 0.6 \left(1 - \frac{f_{ck}}{250} \right) \quad (5.18)$$

where,

N_E & V_E = Axial force and shear force in member, respectively;

μ & c = Parameters depending on roughness of the surface at contact ($\mu = 0.7$ and $c = 0.45$);

S = Ratio of longitudinal force in the new concrete area and the total longitudinal force either in compression or tension zone, both calculated for the section considered;

ϵ = Effectivity factor;

f_{ctd} = Tensile strength of concrete; and

A_c = Cross-sectional area of concrete.

5.5 Seismic design parameters

For seismic resistant design of sandwich panels, the parameters like coefficient of critical damping may be taken as 5% and poisson's ratio as 0.2. Seismic performance factors (SPFs) such as response modification/reduction factor (R-factor), the system over strength factor (Ω_0) and deflection amplification factor (C_d) for sandwich panel construction up to two story building may be taken as $R = 3.5$, $C_d = 3.5$ and $\Omega_0 = 3.0$. Buildings with 4 storey or more do not pass FEMA P695 acceptance criteria (Mashal and Filiatrault, 2012).

5.6 Fire and Durability

RCSP building system also have good resistance against fire. Fire rating of 1.5 hours is obtained by using 1.5 inches thick wythes and 2 hour rating by using 2 inches thick wythes (Mousa, 2014). The fire rating can be further increased by increasing the wythe thickness (Mousa, 2014, Enbuil Manual, 2012a, Enbuil Specification, 2012b). Modified expanded polystyrene used in sandwich panels is non-combustible. It does not contribute to fire and simply melts when exposed to flame. For durability, provisions of IS 456:2000 may be employed.



This page intentionally left blank

CHAPTER 6

Conclusions and Future scope of work

6.1 Conclusions

An experimental study on mechanical behavior of EPS core based RC sandwich panels is conducted. The strength estimated using these tests has been compared with that using the Indian and other codes for ordinary reinforced concrete panels. It is observed that in absence of more rigorous models for EPC-RC composite panels, the models available in codes can be used for estimating the strength with reasonable conservativeness.

The small scale shear and flexure tests have been simulated using Finite Element Analysis. Two models, first using layered shell elements in SAP 200 Nonlinear software and the other using solid (brick) elements for concrete and truss (bar) elements for the reinforcement in ABAQUS have been used. It is observed that the solid element model in ABAQUS yields reasonably accurate simulation of the experimentally obtained load-deflection curve in diagonal compression, but the layered shell element model over-estimates the capacity. In case of the out-of-plane flexure test, initial portion of the load-deflection curve obtained from finite element analysis in ABAQUS matches with the experimental curves, but the latter part of the curves does not match. The results of modelling using layered shell element in SAP 2000 show higher stiffness and strength in comparison to the experimental results.

In addition to the simulation of tests on small scale specimens, detailed analysis of a proposed 4 storey (G+3) building has been performed to study its seismic capacity. Two types of analysis have been performed. First a simple ‘pier analysis’ is performed considering idealized modelling of piers as fixed end vertical frame elements and assuming the spandrels to be rigid. In the second case, a finite element model using layered shell element has been developed in SAP2000 Nonlinear software.

The axial force, bending moment and shear force acting on the critical sections under all the considered load combinations are compared with the capacity. It is observed that the load carrying capacity of the sections is greater than the demand on the sections. The results of



analysis conclude that the design of the building is adequate to withstand the earthquake forces.

Further, the nonlinear analysis shows that the drift demand, in case of the EPS-RC sandwich building is much smaller in comparison with the conventional building systems and is also much lower, even under MCE, than the capacity.

Thus, the tests and analysis performed in this study demonstrate that the EPS core based RC sandwich panel system is a viable construction system for seismically safe buildings.

6.2 Future scope of work

Tests results are promising towards application for load bearing wall building construction. However more full scale testing on junction of wall-wall and wall-slab in sliding shear is needed for having reliable parameters for design.

There is also need for testing of full scale building to study the seismic performance and evaluate factors such as over strength, energy dissipation, damping, stiffness degradation and under in-plane cyclic lateral loading.

There is need to develop definite guidelines or standards for design of sandwich panel components / buildings under gravity and lateral loading.

References

1. Aziz, F. N. A. A., Ali, A. A. A., Jaafar, M. S., Samad, A. A. A., Trikha, D. N., 2004, "Ultimate strength of precast concrete sandwich panel with opening under axial load", *Journal- The Institution of Engineers, Malaysia*, Vol. 65, No. 1 / 2, March/June, pp. 8-12.
2. Bajracharya, R. M., Lokuge, W. P., Karunasena, W., Lau, K.T., Mosallam, A. S., 2012, "Structural evaluation of concrete expanded polystyrene sandwich panels for slab applications", conference paper, proceedings of the 22nd Australasian conference on mechanics of structure and materials, ACMSM22, Sydney, Australia, 11-14th December.
3. Benayoune, A., Samad, A. A. A., Ali, A. A. A., Trikha, D. N., 2007, "Response of pre-cast reinforced composite sandwich panels to axial loading", *Construction and Building Materials*, Vol. 21, pp. 677–685.
4. Benayoune, A., Samad, A. A. A., Trikha, D. N., Ali A. A. A., Akhand, A. M., 2004, "Precast reinforced concrete sandwich panel as an industrialised building system", International Conference on Concrete Engineering and Technology, University of Malaya, Kuala Lumpur, Malaysia.
5. Benayoune, A., Samad, A. A. A., Trikha, D. N., Ali, A. A. A., Ashrabov, A. A., 2006, "Structural behaviour of eccentrically loaded precast sandwich panels", *Construction and Building Materials*, Vol. 20, pp. 713–724.
6. Benayoune, A., Samad, A. A. A., Trikha, D. N., Ali, A. A. A., Ellinna, S. H. M., 2008, "Flexural behaviour of pre-cast concrete sandwich composite panel—experimental and theoretical investigations", *Construction and Building Materials*, Vol. 22 , pp. 580-592.
7. Bournas, D. A., Torrisi, G., Crisafulli, F., Pavese, A., 2012, "Experimental investigation and analytical modelling of prefabricated reinforced concrete sandwich panels", 15th WCEE, LISBOA.
8. Buffarini, G. et al., 2009, "Seismic analysis of EMMEDUE subsystem upon shaking table: Accelerometric readings", Institution for new technology, energy and the environment ENEA-ACS.
9. Bush, T. D. and Stine, G. L., 1994, "Flexural Behavior of Composite Precast Concrete Sandwich Panels with Continuous Truss connectors", *PCI Journal*, Vol. 3 (2), pp. 112-121.
10. Carbonari, G., Cavalaro, S. H. P., Cansario, M. M., Aguado A., 2012, "Flexural behaviour of light-weight sandwich panels composed by concrete and EPS", *Construction and Building Materials*, Vol. 35, pp. 792–799.
11. Carbonari, G., Cavalaro, S. H. P., Cansario, M. M., Aguado, A., 2013, "Experimental and analytical study about the compressive behaviour of EPS sandwich panels", *Materiales de Construcción*, Vol. 63, 311, pp. 393-402.
12. CSI (2010), SAP 2000 Nonlinear, Integrated Software for Structural Analysis and Design-Analysis Reference Manual, Computers and Structures, Inc., Berkeley, California, USA.
13. Desayi, P., and Krishnan, S. (1964). "Equation for the Stress-Strain Curve of Concrete." *ACI Journal Proceedings*, 61(3).



14. Einea, A., Salmon, D. C., Fogarasi, G.J., Culp, T. D., Tadros M. K., 1991. "State-of-the-Art of precast concrete sandwich panels". *PCI Journal*, Vol. 36(6), pp. 78-98.
15. Einea, A., Salmon, D. C., Tadros, M. K., 1994, "A New Structurally and Thermally Efficient Precast Sandwich Panel System", *PCI Journal*, Vol. 39(4), July-August, pp. 90-101.
16. Enbuil, 2012a, Enbuil assembly manual, Revision 4.
17. Enbuil, 2012b, Specification of Enbuil System.
18. EVG-3D, Panel construction system-A brief introduction into the EVG-3D panel construction system.
19. Fam, A. and Sharaf, T., 2010, "Flexural performance of sandwich panels comprising polyurethane core and GFRP skins and ribs of various configurations", *Composite Structures*, Vol. 92, pp. 2927–2935.
20. Forni, M. and Poggianti, A., 2009, "Seismic analysis of EMMEDUE subsystem on vibrating table: Numerical F.E. modelling", Institution for new technology, energy and the environment ENEA-ACS.
21. Gara, F., Ragni, L., Roia, D., Dezi, L., 2012a, "Experimental behaviour and numerical analysis of floor sandwich panels", *Engineering Structures Engineering Structures*, Vol. 36, pp. 258–269.
22. Gara, F., Ragni, L., Roia, D., Dezi, L., 2012b, "Experimental tests and numerical modelling of wall sandwich panels", *Engineering Structures*, Vol. 37, pp. 193–204.
23. "Housing for All by 2022 Mission" – National Mission for Urban Housing , 2015, Ministry of Housing & Urban Poverty Alleviation , Government of India, June 17th
24. Hu, H.-T., Lin, F.-M., and Jan, Y.-Y. (2004). "Nonlinear finite element analysis of reinforced concrete beams strengthened by fiber-reinforced plastics." *Composite Structures*, 63(3–4), 271-281.
25. IS: 1893 (Part 1):2002, "Criteria for earthquake resistant design of structures - Part 1 : general provisions and buildings", *Bureau of Indian Standards*.
26. IS: 456:2000, "Plain and reinforced concrete – code of practice", *Bureau of Indian standard*
27. IS: 875 (Part 3)-1987, "Code of practice for design loads (other than earthquake) for buildings and structures", *Bureau of Indian Standards*.
28. Jankowiak, T., and Lodygowski, T. (2005). "Identification of parameters of concrete damage plasticity constitutive model." *Foundation of Civil and Environmental Engineering*, 06, 53-69.
29. Kabir, M. Z., 2005, "Structural Performance of 3D sandwich panels under shear and flexural loading", *Scientia Iranica*, Vol. 12, No. 4, pp. 402-408.
30. Kadam, S.B. (2015). "Seismic Evaluation and Retrofit of Masonry Buildings." Ph.D. Thesis, IIT Roorkee, Roorkee.
31. Lee, A.J., Kelly, H., Jagoda, R., Rosenfeld, A., Stubee, E., Colaco, J., Gadgil, A., Akbari, A., Norford, L., Burik, H.V., 2006, "Affordable, safe housing based on expanded



- polystyrene (EPS) foam and a cementitious coating” *Journal of Master Science*, Vol. 41, pp. 6908-6916.
32. Mashal, M. and Filiatrault, A., 2012, “Quantification of seismic performance factors for buildings incorporating three-dimensional construction system”, NZSEE Conference.
 33. Mlynarczyk, A. and Pessiki, S., 2000, “Experimental evaluation of the composite behaviour of precast concrete sandwich wall panels”, Center for advance technology for large structural systems (ATLSS), Lehigh University, Report No. 00-07, August, pp. 127.
 34. Mohamad, N., Omar, W. and Abdullah, R., 2011, “Precast lightweight foamed concrete sandwich panel (PLFP) tested under axial load: Preliminary Results”, *Advanced Materials Research*, Vol. 250-253, pp. 1153-1162, Trans Tech Publications, Switzerland.
 35. Mosallam, A. S., 2014, “Structural evaluation of Schnell Home S.R.L. EPS sandwich panel slabs subjected to out-of-plane flexural loads”, SETH-SCHL-FELX0114, Structural Engineering Testing Hall (SETH), Civil & Environmental Engineering Department, The Henry Samueli School of Engineering, University of California, Irvine.
 36. Mourtaja, W., Karadogan, F., Yuksel, E. and Ilaki, A., 2000, 3D behaviour of shotcreted lightweight panel buildings, 12th World Conference on Earthquake Engineering (12WCEE).
 37. Mousa A. and Zidan A., 2014, “3-D Panel System: A sustainable building solution for Egypt”. <http://www.researchgate.net/publication/266208931>, (accessed on 11.12.2015).
 38. Mousa, M. A. and Nasimuddin, 2009, “Experimental and analytical study of carbon fibre-reinforced polymer (FRP)/autoclaved aerated concrete (AAC) sandwich panels”, *Engineering Structures*, Vol. 31, pp. 2337-2344.
 39. Mousa, M. A. and Nasimuddin, 2011, “Global buckling of composite structural insulated wall panels”, *Materials and Design*, Vol. 32, pp. 766–772.
 40. Mowrtage, W. and Karadogan, F., 2009, “Behaviour of Single-Story Lightweight Panel Building under Lateral Loads”, *Journal of Earthquake Engineering*, Vol. 13, pp. 100-107.
 41. Mowrtage, W., 2012, “Low-Rise 3D panel structures for hot regions: Design guidelines and case studies”, *Arab Journal of Science and Engineering*, Vol. 37, pp. 587–600.
 42. Murty C.V.R, 2000, Earthquake Tips (IITK-BMPTC), Learning earthquake design and construction. Indian Institute of Technology Kanpur (IITK) and the Building Materials and Technology Promotion Council (BMTPC).
 43. Mydin, M. A. O., Utaberta, N., Yusof, M. Y. M., Amirudin, N. A., 2015, “Stress-strain relationships of composite foamed concrete panel with different number of shear connectors under compression”, *Jurnal Teknologi (Sciences & Engineering)*, Vol.75:5, pp. 19–25.
 44. Numayr, K. and Haddad, R., 2009, “Static and dynamic analytical and experimental analysis of 3D reinforced concrete panels”, *Structural Engineering & Mechanics*, Vol. 32(3), pp. 399-406.



45. Palermo, M., Gil-Martin, L. M., Hernandez-Montes, E. and Trombetti, T., “2013, In-plane shear behaviour of thin low reinforced concrete panels for earthquake re-construction”, *Materials and Structures*, Vol. 46, pp. 841–856.
46. Palermo, M., Ricci, I., Silvestri, S., Gasparini, G., Trombetti, T., Foti, D., Ivorra, S., 2014, “Preliminary interpretation of shaking-table response of a full-scale 3-storey building composed of thin reinforced concrete sandwich walls”, *Engineering Structures*, Vol. 76, pp. 75–89.
47. Pavese, A., Bournas, D. A., 2011, “Experimental assessment of the seismic performance of a prefabricated concrete structural wall system”, *Engineering Structures*, Vol. 33, pp. 2049–2062.
48. PCI Committee on Precast Sandwich Wall Panels, 1997, “State-of-the-Art of Precast/Prestressed Concrete Sandwich Wall Panels, Second edition” PCI committee report, *PCI Journal*, May-June.
49. PCI Committee on Precast Sandwich Wall Panels, 2011, “State-of-the-Art of Precast/Prestressed Concrete Sandwich Wall Panels” PCI committee report, *PCI Journal*, spring, pp. 131-142.
50. Pessiki, S. and Mlynarczyk, A., 2003, “Experimental Evaluation of the composite behaviour of precast concrete sandwich wall panels”, *PCI Journal*, Vol. 48(2), March-April, pp. 54-71.
51. Poluraju, P. and Rao, G. A., “Influence of longitudinal reinforcement and stiffeners on strength and behaviour of 3D wall panels under axial compression”, jeaconf.org, (accessed on 20.12.2015).
52. Poluraju, P., Rao, G. A., 2014, “Behaviour of 3d-panels for structural applications under general loading: A state-of-the-art”, *International Journal of Research in Engineering and Technology*, Vol. 03, Special Issue 16, pp. 173-181.
53. Refaei, F. A. I., Mihilmy, M. T. E. and Bahaa, T. M., 2015, “Seismic Behavior of Sandwich Panel Walls”, *World Applied Sciences Journal*, Vol. 33 (11), pp. 1718-1731.
54. Rezaifar, O., Kabir, M. Z., Taribakhsh, M., Tehranian, A., 2008, “Dynamic behaviour of 3D-panel single-storey system using shaking table testing”, *Engineering Structures*, Vol. 30, pp. 318–337.
55. Ricci, I., Gasparini, G., Silvestri, S., Trombetti, T., Foti, D., Ivorra-Chorro, S., 2012, “Design of a shaking table test on a 3-storey building composed of cast-in-situ concrete walls”, 15th WCEE, LISBOA.
56. Ricci, I., Palermo, M., Gasparini, G., Silvestri, S., Trombetti, T., 2013a, “Results of pseudo-static tests with cyclic horizontal load on cast in situ sandwich squat concrete walls”, *Engineering Structures*, Vol. 54, pp. 131–149.
57. Ricci, I., Palermo, M., Silvestri, S., Gasparini, G., Trombetti, T., Foti, D., Chorro, S. I., 2013b, “Shake Table Response of a Full-Scale 3-Storey Building Composed of Thin Reinforced Concrete Sandwich walls”, AES-RSESS’2013 First International Conference on Reliability and Safety of Engineering Systems and Structures, Vancouver, CANADA, August 12 – 16.



58. Saheb, S. M. and Desayi, P., 1990, "Ultimate strength of RC wall panels with openings", *Journal of Structural Engineering (ASCE)*, Vol. 116, No. 6, pp. 1565-1578.
59. Sarkar, A., Ahmad, A., Singh, Y., 2016, "Seismic design of expanded polystyrene core panel based building systems", International conference on earthquake engineering and post disaster reconstruction planning, ICEE-PDRP, 24th -26th April, Nepal.
60. Schnell Home, The core wall system Schnell home, by Schnell Wire System.
61. Trombetti, T., Silvestri, S., Gasparini, G., Ricci, I., 2012a, "Results of pseudo-static tests with cyclic horizontal load on H-shaped substructure composed of concrete/polystyrene sandwich bearing panels without openings", *Strategie di sviluppo sostenibile per le costruzioni in Cina, in Europa e in Italia*, pp. 489-498.
62. Trombetti, T., Silvestri, S., Gasparini, G., Ricci, I., 2012b, "Correlations between the experimental results of pseudo-static tests with cyclic horizontal load on concrete/polystyrene sandwich bearing panels and their analytical counterparts", *Strategie di sviluppo sostenibile per le costruzioni in Cina, in Europa e in Italia*, pp. 499-508.
63. Trombetti, T., Silvestri, S., Gasparini, G., Ricci, I., 2012c, "Results of pseudo-static tests with cyclic horizontal load on concrete/polystyrene sandwich bearing panels with and without openings", *Strategie di sviluppo sostenibile per le costruzioni in Cina, in Europa e in Italia*, pp. 509-518.
64. Vecchio, F. (1990). "Reinforced Concrete Membrane Element Formulations." *Journal of Structural Engineering*, 116(3), 730-750.
65. Waryosh, W. A. and Abtan, Y. G., 2013, "Structural behaviour of composite sandwich slab panels", *Journal of Engineering and Development*, Vol. 17, No. 4, October, pp. 220-232.